IN SILICO STUDY OF ALLICIN AND TRIGONELLINE: BIOACTIVITY AND DRUG-LIKENESS THROUGH DFT AND ADMET ANALYSIS

A PROJECT WORK SUBMITTED TO THE
DEPARTMENT OF PHYSICS
TRI-CHANDRA MULTIPLE CAMPUS
INSTITUTE OF SCIENCE AND TECHNOLOGY
TRIBHUVAN UNIVERSITY
NEPAL

FOR THE AWARD OF
BACHELOR OF SCIENCE (B.Sc.) IN PHYSICS

BY
BISHAL BUDHA
SYMBOL NO: 500370248
T.U. REGISTRATION NO: 5-3-37-134-2019

[SEPTEMBER, 2024]

IN SILICO STUDY OF ALLICIN AND TRIGONELLINE: BIOACTIVITY AND DRUG-LIKENESS THROUGH DFT AND ADMET ANALYSIS

A PROJECT WORK SUBMITTED TO THE

DEPARTMENT OF PHYSICS

TRI-CHANDRA MULTIPLE CAMPUS

INSTITUTE OF SCIENCE AND TECHNOLOGY

TRIBHUVAN UNIVERSITY

NEPAL

FOR THE AWARD OF

BACHELOR OF SCIENCE (B.Sc.) IN PHYSICS

BY

BISHAL BUDHA

SYMBOL NO: 500370248

T.U. REGISTRATION NO: 5-3-37-134-2019

[SEPTEMBER, 2024]

RECOMMENDATION

This is to recommend that **Bishal Budha**, Symbol No. 500370248, T.U. Registration No. 5-3-37-134-2019 has carried out project work entitled "***In silico* study of Allicin and Trigonelline: Bioactivity and Drug-likeness through DFT and ADMET analysis**" for the requirement to the project work in Bachelor of Science (B.Sc.) degree in Physics under our supervision in the Department of Physics, Tri-Chandra Multiple Campus, Institute of Science and Technology (IoST), Tribhuvan University (T.U.), Nepal.

To our knowledge, this work has not been submitted for any other degree. He has fulfilled all the requirements laid down by the Institute of Science and Technology (IoST), Tribhuvan University (T.U.), Nepal for the submission of the project work for the partial fulfillment of Bachelor of Science (B.Sc.) degree.

Asst. Prof. Arjun Acharya
Supervisor
Department of Physics
Tri-Chandra Multiple Campus
Ghantaghar, Kathmandu

[15, SEPTEMBER, 2024]

DECLARATION

This project work entitled "***In silico* study of Allicin and Trigonelline: Bioactivity and Drug-likeness through DFT and ADMET analysis**" is being submitted to the Department of Physics, Tri-Chandra Multiple Campus, Institute of Science and Technology (IoST), Tribhuvan University (T.U.), Nepal for the partial fulfillment of the requirement to the project work in Bachelor of Science (B.Sc.) degree in Physics. This project work is carried out by me under the supervision of Asst. Prof. Arjun Acharya , in the Department of Physics, Tri-Chandra Multiple Campus, Institute of Science and Technology (IoST), Tribhuvan University (T.U.), Nepal.

This work is original and has not been submitted earlier in part or full in this or any other form to any university or institute, here or elsewhere, for the award of any degree.

.....

Signature
Name of student: Bishal Budha
Symbol No: 500370248
T.U. Registration No: 5-3-37-134-2019

[15, SEPTEMBER, 2024]

LETTER OF FORWARD

On the recommendation of **Asst. Prof. Arjun Acharya**, this project work is submitted by **Mr. Bishal Budha**, Symbol No. 500370248, T.U. Registration No. 5-3-37-134-2019, entitled "***In silico* study of Allicin and Trigonelline: Bioactivity and Drug-likeness through DFT and ADMET analysis**" is forwarded by the Department of Physics, Tri-Chandra Multiple Campus, for the approval to the Evaluation Committee, Institute of Science and Technology (IoST), Tribhuvan University (T.U.), Nepal.

He has fulfilled all the requirements laid down by the Institute of Science and Technology (IoST), Tribhuvan University (T.U.), Nepal for the project work.

P. B. Adhikari

Dr. Pitri Bhakta Adhikari
Head of Department
Department of Physics
Tri-Chandra Multiple Campus
Tribhuvan University

Head of Department
Physics Department
Tri-Chandra Multiple Campus

BOARD OF EXAMINATION AND CERTIFICATE OF APPROVAL

This project work (PRO-406) entitled "***In silico* study of Allicin and Trigonelline: Bioactivity and Drug-likeness through DFT and ADMET analysis**" by Mr. Bishal Budha, Symbol No. 500370248 and T.U. Registration No. 5-3-37-134-2019 under the supervision of Mr. Arjun Acharya in the Department of Physics, Tri-Chandra Multiple Campus, Institute of Science and Technology (IoST), Tribhuvan University (T.U.), is hereby submitted for the partial fulfillment of the Bachelor of Science (B.Sc.) degree in Physics. This report has been accepted and forwarded to the Controller of Examination, Institute of Science and Technology, Tribhuvan University, Nepal for the legal procedure.

Asst. Prof. Arjun Acharya
Supervisor
Department of Physics
Tri-Chandra Multiple Campus
Tribhuvan University

Dr. Pitri Bhakta Adhikari
Co-Supervisor
Department of Physics
Tri-Chandra Multiple Campus
Tribhuvan University

Dr. Tika Ram Lamichhane
External Examiner
Central Department of Physics
Tribhuvan University

Asst. Prof. Rachana Ghimire
Internal Examiner
Department of Physics
Tri-Chandra Multiple Campus
Tribhuvan University

Dr. Pitri Bhakta Adhikari
Head of Department
Department of Physics
Tri-Chandra Multiple Campus
Tribhuvan University

Head of Department
Physics Department
Tri-Chandra Multiple Campus

[15, SEPTEMBER, 2024]

ACKNOWLEDGEMENT

My heartfelt appreciation goes out to all those whose encouragement, thoughtful guidance, and steadfast assistance made the completion of this thesis possible, I extend my sincere thanks to each one of them.

On the top , I owe my huge gratitude and respect to my supervisor, Assistant Professor Arjun Acharya (Department of Physics, Trichandra Multiple Campus), for his continuous support, encouraging behavior, and invaluable guidance. Despite his hectic schedule, he has been a driving force behind my project. His expertise has illuminated my path in handling the research project, clarifying complex concepts, and addressing critical situations. His constant guidance has been instrumental in completing my work on time. Beyond this project, I am fortunate to have gained many valuable skills and knowledge from him, for which I am also grateful.

I would like to thank Prof. Dr. Rajendra Parajuli and Asst. Prof. Pitambar Shrestha from Amrit Science College (ASCOL), Tribhuvan University (TU), Kathmandu, Nepal, for granting me access to Gaussian software.

I extend my thanks to, Professor Hari Prasad Lamichhane, CDP TU, the Department Head of Physics, Assistant Professor Pitri Bhakti Adhikari, the teaching faculty for their regular inspiration, and to the all the supporting staff of the department for their support throughout completion of this work.

Also, I am also extremely indebted to my friend Shishir Paudel for his valuable support, co-ordination, encouragement, and scholarly advice throughout this project. Additionally, I am deeply grateful to my close friend, Binita Kumari Adhikari, for her support and love during my challenging times.

Ultimately, I want to convey my heartfelt gratitude to my parents and my brothers, Bikash Bikram Budha and Bimal Raj Budha, for providing me with unwavering support and motivation during my time of study and the critical times of exploring and concluding this thesis. They have been a great source of strength and encouragement, and this dissertation is devoted to them, in gratitude for their constant love and support.

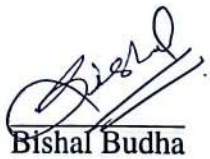

Bishal Budha
Symbol No: 500370248
T.U. Registration No: 5-3-37-134-2019

ABSTRACT

This research has been undertaken to examine the structural, electronic, and vibrational features between two phytochemicals with significant medicinal and therapeutic potential, Allicin and Trigonelline, using a quantum mechanical approach alongside ADMET analysis to assess their drug-likeness and bioactivity. The compounds were optimized by using density functional theory (DFT), employing the B3LYP functional and 6-311++G(d,p) basis set, executing the calculations with Gaussian 16. The optimized structures and parameters of these compounds were then examined, including their electronic characteristics: Frontier orbitals, global reactivity indicators, molecular electrostatic potential of molecules, Mulliken charge distributions, and absorption spectra (UV-Vis), which were yielded with the time-dependent (TD)-DFT method at the identical level of computation while the ADMET evaluation was carried out using SwissADME and ProTox-3.0. The findings revealed that Allicin exhibited higher stability and a larger HOMO-LUMO gap, suggesting lower reactivity compared to Trigonelline, which demonstrated a higher dipole moment and greater electron-donating capacity, making it a strong candidate for antioxidant activity. ADMET analysis indicated that both compounds had suitable lipophilicity, solubility, and gastrointestinal absorption, with Allicin emerging as a more promising drug candidate based on radar plot analysis. Both compounds abided by Lipinski's Rule of Five and exhibited low toxicity, backing their potential as promising drug candidates.

Keywords: Density Functional Theory, Phytochemical, ADMET, HUMO, LUMO

शोधसार

यो अनुसन्धान महत्वपूर्ण औषधीय र चिकित्सीय सम्भाव्यता भएका दुई वनस्पतिमा पाईने रसायन; एलिसिन र ट्राईगोनोलिनको क्वान्टम मेकानिकल दृष्टिकोणलको प्रयोग गर्दै संरचनात्मक, इलेक्ट्रोनिक र भाइब्रेसनल फिचर परीक्षण गर्न र त्यसको साथै तिनीहरूको ए.ड.मि.ई.ट. (ADMET) विश्लेषणको मूल्याङ्कन गर्दै तिनीहरूको औषधी सम्भावयता र जैविक सक्रियताको अध्ययन गर्न गरिएको हो। कम्पाउन्डहरूलाई B3LYP कार्यात्मक र 6-311++ G(d,p) आधार सेटको साथ डेन्सिटि फङ्सनल सिद्धान्त (DFT) प्रयोग गर्दै, गाउसियन १६ सफ्टवेयर प्रयोग गरेर अनुकूलित गरियो। यी यौगिकहरूको अनुकूलित संरचना र प्यारामिटरहरू त्यसपछि जाँच गरियो, तिनीहरूको इलेक्ट्रोनिक गुणहरू सहित: फ्रन्टियर आणविक कक्षाहरू, विश्वव्यापी प्रतिक्रिया वर्णनकर्ताहरू, आणविक इलेक्ट्रोस्टेटिक क्षमता, मुलिकन चार्ज, र अवशोषण स्पेक्ट्रा (UV-Vis), जुन गणनाको एउटै स्तरमा समय-निर्भर (TD)-DFT विधिको साथ प्राप्त भयो। स्विसएडीएमई(SwissAdme) र प्रोटक्स-३.० प्रयोग गरेर ए.ड.मि.ई.ट. मूल्याङ्कन गरिएको थियो। निष्कर्षले एलिसिनले उच्च स्थिरता र ठूलो हुमो(HOMO)-लुमो(LUMO) अन्तर देखाएको छ, जसले निम्न सुझाव दिन्छ; ट्राईगोनोलिनको को तुलनामा एलिसिन कम प्रतिक्रियाशीलता। तर ट्राईगोनोलिन एलिसिनलको तुलनामा उच्च द्विध्रुव क्षण र ठूलो इलेक्ट्रोन-दान गर्ने क्षमता प्रदर्शन गर्दै , एन्टिअक्सिडेन्ट गतिविधिको लागि बलियो उम्मेद्वार देखाएको छ एलिसिन भन्दा। साथै ए.ड.मि.ई.ट. अध्ययन ले यो संकेत गऱ्यो कि दुबै यौगिकहरूमा उपयुक्त लिपोफिलिसिटी, घुलनशीलता, र ग्यास्ट्रोइंटेस्टाइनल अवशोषण छ तर रडार प्लटमा आधारित रहादाँ भने एलिसिन अधिक आशाजनक औषधि उम्मेद्वारको रूपमा उभ्भिएको छन्। दुबै यौगिकहरूले लिपिन्स्कीको पाँच नियमको पालना गरे र अत्यन्तै कम विषाक्तता भएको सावित गर्दै दुवै यौगिकहरूलाई सम्भावित औषधीको उम्मेद्वारहरूको रूपमा निष्कर्ष निकालिएको छ।

मुख्य शब्दहरू: डेन्सिटि फङ्सनल सिद्धान्त, फ्रन्टियर आणविक कक्षाहरू, मुलिकन चार्ज, अवशोषण स्पेक्ट्रा, स्विसएडीएमई

LIST OF ACRONYMS AND ABBREVIATIONS

ADMET:	Absorption, Distribution, Metabolism, Excretion, and Toxicity
DFT:	Density Functional Theory
B3LYP:	Becke, 3-parameter, Lee-Yang-Parr
HOMO:	Highest Occupied Molecular Orbital
LUMO:	Lowest Unoccupied Molecular Orbital
UV-Vis:	Ultraviolet-Visible Spectroscopy
MEP:	Molecular Electrostatic Potential
SMILES:	Simplified Molecular Input Line Entry System
WFT:	Wave Function Theory
BOA:	Born-Oppenheimer Approximation
LDA:	Local Density Approximation
GGA:	Generalized Gradient Approximation
STO:	Slater-Type Orbital
GTO:	Gaussian-Type Orbital
HF:	Hartree-Fock
IR:	Infrared Spectroscopy
NMR:	Nuclear Magnetic Resonance
STEM:	Science, Technology, Engineering, and Mathematics
RMS:	Root Mean Square
LD50:	Lethal Dose for 50% of the population
BBB:	Blood-Brain Barrier
MD:	Molecular Dynamics
LPO:	Lipophilicity
POLAR:	Polarity
INSOLU:	Solubility
FLEX:	Flexibility
INSAT:	Saturation

LIST OF SYMBOLS

μ	Electronic Chemical Potential
I	Ionization Potential Energy
A	Electron Affinity
χ	Electronegativity
η	Chemical Hardness
S	Chemical Softness
ω	Global Electrophilicity Index
E_{total}	Total energy of the system
E_{kin}	Kinetic energy
E_{ext}	External potential energy
E_{Hartree}	Hartree (or Coulomb) energy
E_{xc}	Exchange-correlation energy
$\rho(\mathbf{r})$	Electron density at position $\mathbf{r}$
$V_{\text{ext}}(\mathbf{r})$	External potential
$V_{\text{H}}(\mathbf{r})$	Hartree potential
$V_{\text{xc}}(\mathbf{r})$	Exchange-correlation potential
$\psi_i(\mathbf{r})$	Kohn-Sham orbital functions
ε_i	Kohn-Sham eigenvalues
$\Phi(\mathbf{r})$	Many-body wavefunction
ξ	Exchange-correlation functional
ΔE	Change in energy
$\Delta\rho$	Change in electron density
∇	Gradient operator
∇^2	Laplacian operator
$\hat{T}$	Kinetic energy operator

List of Tables

List of Figures

Contents

CHAPTER 1

1. INTRODUCTION

1.1 General Introduction

Through the ages, natural compounds have been widely used in traditional medicine (Greenwell & Rahman, 2015). Because of their minimal side effects and significant role in early treatments, organic compounds derived from natural sources have offered considerable inspiration in drug discovery (Rishton, 2008; Yafoo et al., 2017) . In the last few decades especially within the realm of computational biophysics as well as computational chemistry, there has been a tremendous upsurge of interest on these organic compounds and their molecular features, reactivity within the body, and their possible uses in therapeutics and medicine through the use of sophisticated computational tools (Wu et al., 2020; Nogrady & Weaver, 2005). Analyzing the active components of folk remedies enables one to deliberate about their practical application for healing ailment and create new forms of modified treatment with the help of those folk remedies or treatment strategies.

1.1.1 Allicin

Sources: Allicin is an organic compound containing sulphur predominantly found in garlic, but it is also present in other plants like garden onions and Savoy cabbage (Block, 1985). It is most abundant in the cloves of garlic and is responsible for the characteristic aroma when garlic bulbs are chopped or crushed (Kourounakis & Rekka, 1991). This compound is produced through the initiation of the enzyme alliinase, which forms Allicin from Alliin when garlic is damaged (Borlinghaus, Albrecht, Gruhlke, Nwachukwu, & Slusarenko, 2014). Allicin also functions as an antifeedant, working as a safeguard against pests preying on the garlic plant (Borlinghaus et al., 2014).

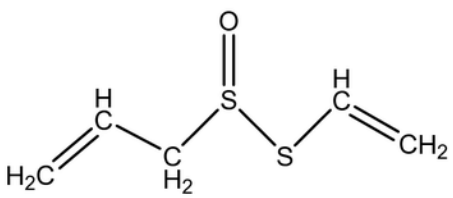

Figure 1: Chemical structure of Allicin.
(Ojha, Tüzün, & Bhawsar, 2020)

Chemical Composition and Structure: Allicin is a thioester derived from sulfenic acid and is chemically identified as diallyl thiosulfinate. The structure of this molecule is characterized by a thiosulfinate group, which contributes to its reactivity and biological activity (Koch & Lawson, 1996). The chemical structure of allicin includes two allyl groups (C_3H_5) attached to a sulfur atom, which is bonded to a sulfinyl group (S=O).

The structure can be represented as:

- **Chemical Structure:** CH_2=CH-CH_2-S-S(=O)-CH_2-CH=CH_2
- **IUPAC Name:** 3-prop-2-enylsulfinylsulfanylprop-1-ene
- **Molecular Formula:** $C_6H_{10}OS_2$
- **Molecular Weight:** 162.27 g/mol

Biological Significance: Allicin contains a thiosulfinate functional group, which is highly reactive and imparts oxidizing abilities. It can oxidize thiols present in cells, including glutathione and cysteine, which are considered residues in proteins. This reactivity is believed to be critical for its biological activity and contributes to its antioxidant properties (Gruhlke & Slusarenko, 2012). It could boost the immune system, aiding the body in combating illnesses and infections more effectively. It poses broad-spectrum antimicrobial properties (Choo et al., 2020), being effective against bacteria, fungi, and viruses. It can restrict the growth of strains resistant to antibiotics like *Staphylococcus aureus*, making garlic a traditional remedy in many cultures for treating infections (Borlinghaus et al., 2014). It functions as an antioxidant by neutralizing free radicals and mitigating oxidative stress (Chan, Yuen, Chan, & Chan, 2013). It has exposed itself with potentiality to lower cholesterol levels, minimizing platelet aggregation, and lessening blood pressure, all of which contribute to improved cardiovascular health (García-Trejo et al., 2016). It can promote programmed cell death in cancer cells and suppress their growth (Y. Zhou et al., 2022). At sub-lethal concentrations, it provides various health benefits, including supporting cardiovascular health and potentially offering protective effects against certain diseases (Gao et al., 2024). It is a vital compound derived from garlic, possessing significant biological importance due to its range of human health benefiting properties, including antioxidant, antimicrobial, anti-inflammatory, anticancer, and antidiabetic (Saikat et al., 2021; Gao et al., 2024).

1.1.2 Trigonelline

Sources: Trigonelline, also known as Caffearine, is a naturally occurring alkaloid derived from the amino acid tryptophan. It is a dipolar ion formed through the methyl modification of the nitrogen atom in niacin (vitamin B3), and consequently acts as a byproduct from vitamin B3 metabolism (Ouzir, El Bairi, & Amzazi, 2016). It is widely distributed in multiple

plants, such as coffee beans, fenugreek seeds, garden peas, hemp seeds, oats, and some legumes (Henry Anderson, 1949). It is particularly abundant in Arabica coffee.

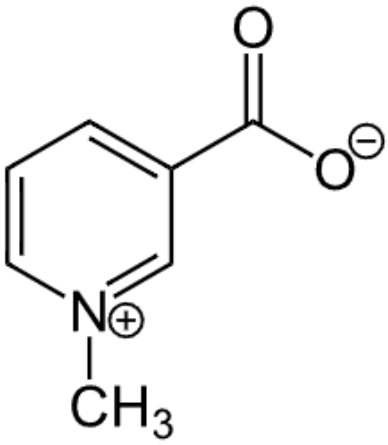

Figure 2: Chemical structure of Trigonelline (Yarnell, 2015).

Chemical composition and structure: Trigonelline features a distinctive chemical structure consisting of a pyridine ring with a methyl group and a carboxamide group attached. The six-membered pyridinium ring includes five carbon atoms and one nitrogen atom, with a carboxylate group (-COO) on the third carbon to balance the nitrogen's positive charge.

The structure is represented as follows:

- **Chemical Structure:** $CH_3\text{-}N^+(CH_2)_3\text{-}COO^-$
- **IUPAC Name:** 1-methylpyridin-1-ium-3-carboxylate
- **Molecular Formula:** $C_7H_7NO_2$
- **Molecular Weight:** 137.14 g/mol

Biological Significance: The hypoglycemic effects of Trigonelline are scientifically attributed to its insulin-comparable effects on human system, given that it lowers blood sugar levels, so it may be of great interest to diabetics (Aktar, Ferdousi, Kondo, Kagawa, & Isoda, 2024). The material has shown potential for eradicating cancer through halting of cancer cell proliferation, induction of apoptosis and overcoming chemo-resistance, all without severe side effects (Raymond Tice, 2000). It is also found that it can act as an anti-inflammatory and antimicrobial to fight inflammation and bacterial and viral infections in the body (J. Zhou, Chan, & Zhou, 2012). It has the anti-oxidant activity that may aid in the reduction of cellular damage. Protection of the brain and a possible enhancement of the learning and memory may be achieved by

the decrease of the pro-inflammatory cytokines and increase in the release of neurotransmitters such as Trigonelline (Daglia, Cuzzoni, & Dacarro, 1994). Furthermore, it is crucial for various short-term and long-term processes associated with plant growth and development. In plants, it is involved in halting the cell cycle during the G2 phase and may function as a signal transducer in response to oxidative stress (Daglia et al., 1994). In addition, it is utilized in a number of metabolic reactions in different plants as well as nitrogen metabolism, and is used up in the synthesis of niacin (vitamin B3) in certain species (Nguyen, Taine, Meng, Cui, & Tan, 2024). Being the bio active compound, it exhibits great prospect in medicine, nutrition and agriculture.

With significant potential across medicine, nutrition, and agriculture, it is a noteworthy bio-active compound.

1.1.3 ADME characteristics and Toxicity:

ADME refers to the processes of Absorption, Distribution, Metabolism and Excretion that define interaction within the body of the drugs or substances. These characteristics impact on the function and pharmacology of a compound as a drug and it levels and disposition kinetics in tissues and target organs (Tetko, Bruneau, Mewes, Rohrer, & Poda, 2006). The assessments of ADME characteristics are critical concerning the drug development process because they determine its safety and effectiveness (Tetko et al., 2006). Distribution is the process through which a compound moves from place to another in the body, especially into the bloodstream us, from the site of administration, and the factors influencing this process include presence of food in the stomach, the formulation of the compound itself and its chemical characterizations like solubility and permeability, among others. After absorption, distribution takes place, in this process the substance goes with the blood stream to other tissues and organs in the body. Some of the parameters that define this phase include the flow rate of blood, molecular size, cell membrane permeability and binding of the compound to plasma proteins particularly albumin. It mainly occurs in the liver where enzymes work to make alterations on the compound and release products referred to as metabolites. Through this process the drugs activity may be changed and the chemical gets ready for excretion. Metabolism depends among other things on genetics, interactions with other drugs, the patients age, and overall heath condition. Last of all, metabolism includes the elimination of a drug and its metabolites from the body normally in urine, feces, sweat or breath. Urine elimination is of great importance in order to avoid accumulation of such substances. ADME factors are pivotal in assessing the pharmacokinetics of drugs and the general impact it beholds to the body, a major concern to the realisation of the efficacy and safety of therapeutic agents. This understanding also applies to the correct dosage, frequency of administration, method of administration and the possibility of interaction with other drugs (Balani, Miwa, Gan, Wu, & Lee, 2005).

Toxicity is the measure of extent of the effect that a chemical compound has on the human body

in its interaction with the chemical compound. In toxicity assessment execution, the assessment of the adverse impacts of a substance on life forms is usually considered.

1.2 Rationale

Over the past few decades, there has been a significant increase in interest in identifying various biochemical compounds for their medicinal and therapeutic properties.This trend is focused on identifying and characterizing natural chemicals from plants, marine organisms, and microbes, and analyzing their potential health benefits and efficacy as drugs. The sophistication of technology, including computational methods in the realms of biotechnology, biophysics, and medical chemistry, has fueled the study of molecular bioassays, genetics, proteomics, and theoretical computational methods at high speeds, paving the way toward the discovery and development of novel medicinal compounds. The combined efforts of chemists, biologists, physicists, pharmacologists, and medical science experts have advanced the understanding of how these compounds interact with living organisms and their impact on human health.

The primary reasons for this increased interest are; the crucial need for effective treatments for cancer, tumors, neurological disorders, and other chronic diseases such as diabetes, hypertension, increased cholesterol, uric acid, and others that have been spreading like a pandemic (Wani et al., 2022). Other reasons include the different chemical structures of natural products compared to synthetic ones, and the consideration and preference for natural products because they are safer for the environment and consumer use (Wani et al., 2022). Considering this, this study aims to compare two phytochemical compounds, Allicin and Trigonelline, derived from widely consumed daily foods, which will surely add some impacts on the research rush for finding biological medicinal alternatives of such chronic diseases.

Allicin offers significant medical benefits such as antihypertensive and antimicrobial properties, while Trigonelline has shown strong antidiabetic effects (Gao et al., 2024; Aktar et al., 2024). Both compounds have been found to have common clinical applications in antioxidant, anti-inflammatory, anticancer, and neuroprotective contexts (Borlinghaus et al., 2014; Gao et al., 2024). This research will conduct a comparative DFT analysis to study their molecular effects and aid in designing improved therapeutic agents. Comparing the stability and reactivity of allicin and trigonelline will help assess which compound might be more effective or safer in biological systems. Within DFT, this research focuses on properties such as Dipole moment, HOMO-LUMO gaps, MEP, Mulliken charges, vibrational and absorption analysis, which are crucial parameters for determining polarity, permeability, reactivity, stability, possible targeted sites, and mechanisms of action (Adekoya, Adekoya, Sadiku, Hamam, & Ray, 2022). All these factors are essential for identifying the potential of these compounds as drugs. Both compounds are known for their antioxidant activity (Daglia et al., 1994; Gruhlke & Slusarenko, 2012), which is crucial for combating oxidative stress-related diseases. This study will contribute in

identifying their favorable electronic structures for antioxidation and their redox potentials to determine which one is more efficient in its antioxidant mechanisms.

Furthermore, ADMET evaluation will reveal which of the two compounds can be efficiently absorbed, distributed, metabolized, and excreted by the human body, which is crucial information for determining the effectiveness of a compound to be a drug (Tetko et al., 2006). Additionally, it is essential to assess toxicity to detect possible negative impacts and ensure safety. This comparative study using DFT and ADMET aims to provide a comprehensive understanding of both compounds, assisting in identifying their potential therapeutic and medicinal value and suitability for specific biological targets according to various diseases.

Therefore, the findings of this research could assist to understand the alignment of its quantum mechanical and ADMET properties with biological significance of these compounds, their properties to be drug candidates and help to enhance the specific field of medicine with the help of these phytochemicals.

1.3 Objectives

The primary goal of this dissertation is to conduct an inclusive comparative study about the electronic properties, ADME characteristics, and toxicity profiles of allicin and trigonelline using advanced computational methods. This study aims to reveal clear insights in the potential applications and safety profiles of these compounds, which are significant in various fields such as biophysics and medicinal chemistry.

1.3.1 General Objective

- To carry out Density Functional Theory (DFT) analysis of Allicin and Trigonelline using Gaussian software, applying the Becke 3-parameter, Lee-Yang-Parr (B3LYP) functional with the 6-311++G(d,p) basis set, along with an ADMET analysis

1.3.2 Specific Objectives

1. To conduct a DFT study of Allicin and Trigonelline to:
    - Determine the optimized molecular structures of both compounds
    - Analyze their electronic properties; Dipole moment, Mulliken Charge, Molecular electrostatic potential, Global reactivity descriptors, including HOMO-LUMO energy gaps
    - Analyze the stability and reactivity of these compounds through computational methods based on these above calculations

2. To examine the ADME (absorption, distribution, metabolism, and excretion) characteristics of Allicin and Trigonelline using SwissADME to:
    - Predict the lipophilicity, permeability, and solubility of both compounds
    - Evaluate the pharmacokinetic profiles of these compounds and their druglikeness
3. To assess the toxicity of Allicin and Trigonelline using ProTox to:
    - Assess and compare the toxicity profiles of Allicin and Trigonelline
    - Identify any potential toxic effects and safety concerns associated with these compounds
4. To compare the overall biological activity and potential therapeutic applications of allicin and trigonelline based on the DFT, ADME, and toxicity results

By achieving these objectives, this study aims to deliver valuable knowledge to the field of computational biophysics, providing a foundation for future research and potential therapeutic applications of Allicin and Trigonelline.

CHAPTER 2

2. LITERATURE REVIEW

Numerous researchers have studied these compounds quantum mechanically using both experimental and computational methods. I have reviewed the following literature during my study because it provides a clear understanding of my research efforts:

Muhhamad et al. (2007) studied on Allicin and other bioactive constituents in garlic and based on his findings he concluded that it increases antimicrobial, anticancer, antioxidant effects, decreases cardiovascular diseases as well as improve immune and anti-diabetic effects (Rahman, 2007).

Allred et al. (2009) studied Trigonelline, concluding that it it encourage antidiabetic activity, anticancer activity, antioxidant activity and the ability to minimize occurrence of cardiovascular diseases (Allred, Yackley, Vanamala, & Allred, 2009).

Ting and Danzhi (2010) researched the uses of quantum mechanics in drug designing and highlighted the vast significance of DFT in drug design, including its contribution in choosing the chemicals for the drugs (T. Zhou, Huang, & Caflisch, 2010).

Faik Gökalp (2018) carried out a DFT study of Allicin together with other garlic-derived compounds using the Gaussian 09 software with B3LYP functional and 6-31G(d,p) basis sets. The study found that allicin has a Gibbs free energy of -1106.104763 hartree, indicating its thermodynamic stability in biological environments. The HOMO energy of -0.25650 eV suggests a moderate electron-donating capability, while the LUMO energy of -0.06745 eV reflects its ability to accept electrons. The HOMO-LUMO gap of 0.18905 eV points to balanced chemical reactivity, and the dipole moment of 4.3439 Debye indicates suitable polarity for effective interactions with biological targets (Gökalp, 2018).

Rodriguez-Clemente et al. (2017) studied Allicin through both experimental and DFT theoretical methods, using the B3LYP functional and 6-311G(d,p) basis set. They found that allicin can adsorb via oxygen and sulfur atoms, with E_{LUMO} and E_{HOMO} values indicating a strong tendency to donate electrons, linking its electronic properties to its efficiency. The presence of water increased allicins chemical reactivity, as seen in less negative E_{LUMO} values, highlighting its propensity to donate electrons. The study also showed differing electron affinity (EA) between gas and solvent phases, with positive EA in water. Optimized parameters were computed and compared with data from the literature. (Rodriguez-Clemente et al., 2017).

Yavuz et al. (2023) conducted DFT-based quantum chemical computations on allicin with the help of the Gaussian 09W program using B3LYP/6-31++G(d,p) basis set. The study found that

Allicin has a strong electron-donating tendency, with a LUMO-HOMO diffrence of 5.06837 eV in gas and 5.21504 eV in water, indicating high energy needs for electron transfer. MEP analysis revealed electrophilic regions on sulfur atoms, suitable for nucleophilic attacks. Allicins quantum descriptors showed high reactivity and low stability. ADMET characteristics were assessed using tools like ADMETlab, admetSAR, SwissADME, ProTox-II, and SwissTargetPrediction, confirming allicins favorable drug-like properties without toxicity or carcinogenicity (Yavuz, n.d.).

Babatunde Joseph et al. (2022) conducted pharmacoinformatics studies on Allicin, evaluating its pharmacokinetics, including lipophilicity, water solubility, and gastrointestinal absorption. Allicin exhibited good water solubility and high gastrointestinal absorption, suggesting its suitability for oral administration. Additionally, it showed potential to cross the blood-brain barrier, indicating that further toxicity evaluation is necessary. Virtual toxicological assessments indicated that allicin has moderate toxicity with an LD50 value of 874 mg/kg, but it does not pose significant risks for hepatotoxicity, carcinogenicity, or mutagenicity, making it a promising candidate for therapeutic use (Oso, Adeoye, & Olaoye, 2022).

Rashmi Ranjan (2023) evaluated Trigonelline and other phytochemicals for their potential in diabetes management. They used chemical databases to obtain 2D structures and SMILES formulas and assessed drug-likeness properties. Trigonelline, with a molecular weight of 137.14 Da and a logP value of 0.14, met drug-likeness criteria, indicating favorable properties. Pharmacokinetic analysis showed high gastrointestinal absorption and minimal blood-brain barrier crossing for trigonelline. The study concluded that trigonelline, alongside Andrographolide, demonstrated significant therapeutic potential with low toxicity, suggesting it is a promising candidate for diabetes treatment (Ranjan, Choudhary, Singh, et al., 2023).

Gap in the Research: Although there is a few number of DFT studies conducted on Allicin only, Trigonelline is relatively less explored compared to other phytochemicals. Additionally, there is a lack of comparative DFT studies between Allicin and Trigonelline. This study aims to address the limited exploration of trigonelline and the absence of comparative analysis of these chemicals by conducting a comparative DFT study, along with incorporating ADMET analysis.

CHAPTER 3

3. MATERIALS AND METHODS

3.1 Theoretical Background

To fully and precisely characterize the electronic system , the quantum mechanical method is the only one that can be applied (Jensen, 2007). According to quantum mechanics, the wave function can be used to determine a system's observable properties. In other words, the wave function provides valuable information about molecules, including dipole moments, polarizability, and more (Sherrill, 2000). Thus, in principle, the molecular structure and its chemical reactivity can be quantitatively predicted at a precise level by implementing the Schrödinger equation. However, in fact, this objective is challenging to achieve due to mathematical and computational diffculty, symboling the use of approximate techniques (Hehre, Ditchfield, & Pople, 1972).

To understand chemical problems, methods based on either wave function theory (WFT) or density functional theory (DFT) can be employed. The *ab initio* method is a non-empirical computational approach used to estimate the structural and electronic properties of molecules. Essentially, all quantum mechanical methods begin with the Schrödinger equation as their foundational basis (Hehre et al., 1972). It is used to obtain the properties of non-relativistic quantum systems from the given equation (Schrödinger, 1926):

$$\hat{H}\Psi(R,r) = E\Psi(R,r) \tag{3.1}$$

For a molecular system with N electrons and M nuclei, the Hamiltonian can be represented as:

$$\hat{H} = -\frac{\hbar^2}{2m_e}\sum_{i=1}^{N}\nabla_i^2 - \sum_{U=1}^{M}\frac{\hbar^2}{2M_U}\nabla_U^2 + \frac{1}{2}\sum_{i\neq j}\frac{e^2}{|\mathbf{r}_i - \mathbf{r}_j|} - \frac{1}{2}\sum_{i,U}\frac{Z_U e^2}{|r_i - R_U|} + \frac{1}{2}\sum_{U\neq V}\frac{Z_U Z_V e^2}{|R_U - R_V|} \tag{3.2}$$

Where,
$M_U = U^{th}$ nucleus mass
$e =$ electron charge
$m_e =$ electron mass

The summation with U, V stands for nuclei and i, j stands for electrons. In this equation 3.2, the first two terms represent the kinetic energies of the electrons and nuclei. The remaining three terms include the attractive electrostatic potential between the electrons and nuclei, while the last two terms account for the repulsive potentials between electron-electron and nucleus-nucleus interactions.

The Schrödinger equation can only be completely solved for a single-particle system., but for a two-electron or many electron system it cannot be solved exactly, so an approximation is needed to be introduced. The *ab initio* (or first principles) approach, which is non-empirical, is employed to accurately address the many-body problem. These calculations use the correct Hamiltonian that depends on only the fundamental physical parameters. A commonly used method is the Hartree-Fock Self-Consistent Field (SCF), *ab initio* calculation, which employs an anti-symmetrized wave function.

3.1.1 Born-Oppenheimer approximation (BOA)

The pioneer approach required to simplify the Schrödi-nger equation is considered for Born-Oppenheimer approximation the pioneer approach required to simplify the Schrödi-nger equation.In a many-body system, the interactions among electrons become more intricate and intensify with the increasing number of electrons. Hence, to reduce the complexity, the electronic and nuclear parts are taken diffrently .The masses of the nuclei are several times greater than those of the electrons. Consequently, as noted by Born and Oppenheimer (1927), the kinetic energy of the nuclei is negligible compared to that of the electrons, and the nuclear-nuclear Coulomb repulsion can be considered constant. Now, the wave function can be interpreted as

$$\Psi(R,r) = \phi(R)\chi(r,R) \tag{3.3}$$

where $\phi(R)$ denotes the wave function of the nucleus, and $\chi(r,R)$ represents the wave function of the electron. The Schrödinger equation for the electronic part is as follows:

$$\hat{H}_{el}\chi(r,R) = E_{el}\chi(r,R) \tag{3.4}$$

where, the electronic Hamiltonian is,

$$\hat{H} = -\frac{\hbar^2}{2m}\sum_{i=1}^{N}\nabla_i^2 + \frac{1}{2}\sum_{i\neq j}\frac{e^2}{|\mathbf{r}_i - \mathbf{r}_j|} - \frac{1}{2}\sum_{i,U}\frac{Z_U e^2}{|r_i - R_U|} \tag{3.5}$$

After adding the constant repulsion term(V_{NN}):, the total energy of the system is

$$E_{tot} = E_{el} + V_{NN} \tag{3.6}$$

$$V_{NN} = \frac{1}{2} \sum_{U \neq V} \frac{Z_U Z_V e^2}{|R_U - R_V|} \tag{3.7}$$

$$H_\phi(R) = E_\phi(R) \tag{3.8}$$

Solving these two equations provides the total energy of the system.

3.1.2 Hatree-Fock approximation

The BOA approximation simplifies the Schrödinger equation, separating the Hamiltonian into two parts: electronic and nuclear. However, the Schrödinger equation is still unsolvable due to the inter-electronic repulsion term, $\frac{1}{2}\sum_{i \neq j} \frac{e^2}{|\mathbf{r}_i - \mathbf{r}_j|}$. The distance between electrons is difficult to measure since their motions are correlated (Jensen, 2007).

Hartree and Fock solved the problem by considering electrons with no correlation. According to the independent particle approximation introduced by Hartree (1928) (Hartree, 1928), a one-electron molecular orbital (wave function) is assumed that each electron is influenced by the average effective field created by the nuclei and all other remaining electrons. This assumption is made for each electron, and the total wave function of the electrons in a many-body system is approximately expressed as the product of N one-electron wave functions, as follows:

$$\Psi(\mathbf{r}_1, \mathbf{r}_2, \ldots, \mathbf{r}_n) = \chi_1(r_1)\chi_2(r_2)\ldots\chi_n(r_n) \tag{3.9}$$

It is referred to as a Hartree product. The energy of the system is subsequently estimated using this wave function in the following manner::

$$H\Psi(\mathbf{r}_1, \mathbf{r}_2, \ldots, \mathbf{r}_N) = E\Psi(\mathbf{r}_1, \mathbf{r}_2, \ldots, \mathbf{r}_N) \tag{3.10}$$

Since the wave function $\Psi(\mathbf{r}_1, \mathbf{r}_2, \ldots, \mathbf{r}_N)$ derived from the Hartree product does not agree the anti-symmetry property, it fails to describe fermions. Moreover, to incorporate the exchange and correlation terms, Hartree's method was further improved using the anti-symmetric nature of electrons by Fock (1930). As a consequences, the approach is called as the Hartree-Fock (H-F) approximation (Hartree, 1928). In the Hartree-Fock approximation, the wave functions are arranged in a single Slater determinant for N spin-orbitals (Slater, 1937):

$$\Psi = \frac{1}{\sqrt{N!}} \begin{vmatrix} \chi_1(r_1,s_1) & \chi_2(r_1,s_2) & \cdots & \chi_n(r_1,s_n) \\ \chi_1(r_2,s_1) & \chi_2(r_2,s_2) & \cdots & \chi_n(r_2,s_n) \\ \vdots & \vdots & \ddots & \vdots \\ \chi_1(r_n,s_1) & \chi_2(r_n,s_2) & \cdots & \chi_n(r_n,s_n) \end{vmatrix} \tag{3.11}$$

This is the anti-symmetrized wave function which is used to describe electrons. Now the energy expression is resulted by,

$$(E_{el}) = \langle \Psi | \hat{H} | \Psi \rangle \tag{3.12}$$

The appropriate approximate wave function that corresponds to the minimum energy can be determined using the variational theorem. Now, the Hartree-Fock energy expression is

$$E^{HF} = \sum_u \langle \Psi | h | \Psi \rangle + \frac{1}{2} \sum_{uv} [uu|vv] - [uv|vu] \tag{3.13}$$

where, for one-electron integral

$$\sum_u \langle \Psi | h | \Psi \rangle = \int dx_1 \Psi_1^*(x_1) h(r_1) \Psi_x(x_1)$$

and for two-electron integral

$$[uv|wx] = \int dx_1 dx_2 \Psi_u^*(x_1) \Psi_v(x_1) \frac{1}{r_{12}} \Psi_w^*(x_2) \Psi_x(x_2)$$

Now, after minimizing and simplifying the Hartree-Fock energy expression, we get

$$h(x_1)\Psi_u(x_1) + \sum_{v \neq u} \left[\int dx_2 |\Psi_v(x_2)|^2 \frac{1}{r_{12}} \right] \Psi_u(x_1) - \sum_{v \neq u} \left[\int dx_2 \Psi^*(x_2) \frac{1}{r_{12}} \right] \Psi_u(x_1) = \varepsilon_u \Psi_u(x_1) \tag{3.14}$$

where, ε_Ψ is the energy related to Ψ_u, the initial term in the equation above that is

$$\sum_{v \neq u} \left[\int dx_2 \, |\Psi_v(x_2)|^2 \frac{1}{r_{12}} \right] \Psi_u(x_1)$$

is the Coulomb force of electrons and the next part

$$\sum_{v \neq u} \left[\int dx_2 \, \Psi^*(x_2) \frac{1}{r_{12}} \right] \Psi_u(x_1)$$

is the exchange term (Sherrill, 2000).

Moreover, The HF approximation could not take the consideration for the correlation effect of the electrons. It overestimates the total energy. Correlation is the coupling of electron motions that decrease the electron-electron repulsion energy. Thus, correlation given the difference between the Hartree-Fock energy and actual energy of the system (Hehre et al, 1972). Further, many methods such as MP2, MP3, MP4, etc. were developed to account the correlated molecular system (Hehre et al, 1972).

Correlated molecular system (Harrison, 2003). However, these methods rely on the wave function and these wave function consists the $4N$ coordinates system: $3N$ space coordinates and N spin coordinate. Thus, it requires a large computational cost for a huge system. In contrast, the density functional theory (DFT) method is grounded in the density of the electrons. Since the electron density depends on only $3N$ space coordinates, it requires less computational cost (Harrison, 2003; Baseden & Tye, 2014). Hence, it has become more widely used to address many-body problems.

3.2 Density functional theory (DFT)

DFT is the most frequently employed quantum theory for determining the electronic structure of molecules, relying on the electron density $\rho(\mathbf{r})$ not in many electron wave function $\Psi(\mathbf{r}_1, \mathbf{r}_2, \ldots)$. It is applied to compute electronic ground state energy in terms of electron density. It has become the method of choice for theoretical physicists and chemists for determining the structures, surfaces, defects, and electrical properties of solids over the last three decades . The base of the DFT lies on the two theorems proposed by Hohenberg and Kohn (Kohn & Sham, 1965)) and on the Kohn-Sham approximation (Hohenberg & Kohn, 1964). These can be stated as follows:

3.2.1 Hohenberg-Kohn Theorem

Hohenberg-Kohn has been expressed in two theorems:

Theorem first: It states that "the ground state density determines the external potential uniquely".

$$\rho(\mathbf{r}) \rightarrow V(\mathbf{r}) \tag{3.15}$$

If for any electron body, the density $\rho(\mathbf{r})$, potential $V(\mathbf{r})$ and $V'(\mathbf{r})$ are associated to the N-ground state different external potential H and be the respective Hamiltonian

$$H = T + U + V_{ee}, \quad H' = T + U' + V'_{ee} \tag{3.16}$$

where,

$$T = -\frac{1}{2}\sum_{i=1}^{N}\nabla_i^2$$
$$U = \frac{1}{2}\sum_{i\neq j}\frac{1}{|r_i - r_j|}$$

The term defining interaction between electron-elctron is given by:

$$V_{ee} = \sum_i V(r_i)$$

$$V'_{ee} = \sum_i V'(r_i)$$

If the energy linked with Ψ and Ψ' are E and E' correspondingly, then, utilizing the variational principle,

$$E = \langle\Psi|H|\Psi\rangle \leq \langle\Psi|H'|\Psi'\rangle \tag{3.17}$$
$$\leq \langle\Psi|H'|\Psi'\rangle + \langle\Psi|H - H'|\Psi'\rangle \tag{3.18}$$
$$\leq E' + \int dr\,\rho(r)\left[V(\mathbf{r}) - V'(\mathbf{r})\right] \tag{3.19}$$

and

$$E' = \langle\Psi'|H'|\Psi'\rangle \leq \langle\Psi|H'|\Psi\rangle \tag{3.20}$$
$$\leq \langle\Psi|H|\Psi\rangle + \langle\Psi|H' - H|\Psi\rangle \tag{3.21}$$
$$\leq E + \int dr\,\rho(r)\left[V'(\mathbf{r}) - V(\mathbf{r})\right] \tag{3.22}$$
$$E' \leq E + \int dr\,\rho(r)\left[V'(\mathbf{r}) - V(\mathbf{r})\right] \tag{3.23}$$

Summing Equations 3.19 to 3.23, it becomes

$$E + E' \leq dE + dE' \tag{3.24}$$

which is a contradiction. Hence, the theorem is verified by reductio ad absurdum

Theorem second: It states that "the universal functional $F[\rho_0(r)]$, gives the true ground state energy E_0 when $\rho(r)$ is the true minimum energy density for the initial density is the true

ground state density". To the provided external potential $V_{ex}(r)$, energy is defined as

$$E^{\mathrm{HK}}[\rho(r), V_{ex}] = T[\rho(r)] + V_{ee}[\rho(r)] + \int V_{ex}(r)\rho(r)dr \tag{3.25}$$

where, the initial, second and third part in right hand side respectively represents kinetic energy due to electron-nuclei interactions $(K.E.)$, Coulomb potential energy of interacting electrons and external potential energy i.e. because of interactions between electron and nuclei. Then,the universal functional, $F[\rho(r)]$, is given as

$$F(\rho) = T[\rho(r)] + V_{ee}[\rho(r)] \tag{3.26}$$

E(ρ) is assumed to be minimum energy for exact density, where

$$N = \int \rho(r)dr \tag{3.27}$$

Now, the above equation can be written as $F[\rho(r)]$ is stated as

$$E^{\mathrm{HK}}[\rho(r), V_{\mathrm{ex}}] = F[\rho(r)] + \int V_{\mathrm{ex}}(r)\rho(r)\,dr \tag{3.28}$$

From the principle of minimal

$$E[\rho(r), V_{\mathrm{ex}}] \geq E[\rho_0(r), V_{\mathrm{ex}}] = E \tag{3.29}$$

The exact ground parameters are obtained by minimizing above with respect to electron density. Nevertheless, obtaining exact energy functional is challenging since it is concerned with the Kinetic energy associated with the electrons. The $F[\rho(r)]$, is further solved by employing Kohn-Sham approach (Kohn & Sham, 1965).

3.2.2 Kohn-Sham approach

Accurately determining the kinetic energy related to density remains challenging. However, it is easy to calculate in terms of wavefunction. Thus, Kohn & Sham (1965) considered an interacting electronic system to a non-interacting such that it gives the exact density of the real interacting system . The K-S stated the universal functional as follows (Kohn, Becke, & Parr, 1996):

$$F[\rho(r)] = T_s[\rho(r)] + J^H[\rho(r)] + E_{\mathrm{XC}}[\rho(r)] \tag{3.30}$$

In expression given above, where

$$T_s[\rho(r)] = \text{K.E. for non-interacting particle}$$

$$J^H[\rho(r)] = \frac{1}{2}\iint \frac{\rho(r_i)\rho'(r_j)}{|r_i - r_j|} dr_i dr_j$$

$$= \text{energy resulting from the electrons' coulomb electrostatic interaction}$$

$$E_{\text{XC}}[\rho(r)] = \text{exchange-correlation energy}$$

Also, E_{XC} is stated as,

$$E_{\text{XC}} = \Delta T[\rho] + \Delta V[\rho]$$

Where'

$$\Delta T[\rho] = T[\rho] - T_s[\rho]$$

$$\Delta V[\rho] = V_{\text{ee}} - J^H[\rho(r)]$$

Now, the energy functional can be written as

$$E[\rho] = T_s[\rho] + \int V_{\text{ex}}(r)\rho(r)dr + J^H[\rho(r)] + E_{\text{XC}}[\rho(r)] \tag{3.31}$$

where, $T_s[\rho(r)] = \sum_i^N \int \psi_i^* \left(-\frac{1}{2}\nabla^2\right) \psi(i)dr$

The minimum energy is obtained by differentiating the total energy corresponding to electron density, $\rho(r)$ i.e. $\delta[E(\rho)] = 0$. Now, the Kohn-sham equation is derived using lagrange undetermined multipliers method employing constrain as follows:

$$\delta[E(\rho) - \lambda N] = 0 \tag{3.32}$$

$$\int \frac{\delta}{\delta\rho(r)}[E(\rho) - \lambda N]\delta\rho(r)dr = 0 \tag{3.33}$$

where, λ = lagrange multiplier and constrain is $\int \rho(r)dr = N$

$$\int \frac{\delta T_s[\rho(r)]}{\delta\rho(r)}\delta\rho(r)\,dr + \int \frac{\delta V_{\text{ex}}(r)\rho(r)}{\delta\rho(r)}\delta\rho(r)\,dr + \int \frac{\delta}{\delta\rho(r)}\left[\frac{\rho(r)\rho'(r_j)}{|r-r'|}\right]\delta\rho(r)\,dr'\,dr + \int \frac{\delta E_{\text{XC}}[\rho(r)]}{\delta\rho(r)}\delta\rho(r)\,dr - \lambda\int \frac{\delta\rho(r)}{\delta\rho(r)}\delta\rho(r)\,dr = 0 \tag{3.34}$$

$$\int \left[\frac{\delta}{\delta\rho(r)}T_s[\rho(r)] + V_{\text{ex}}(r) + \int \frac{\rho(r')}{|r-r'|}dr' + \frac{\delta E_{\text{XC}}[\rho(r)]}{\delta\rho(r)} - \lambda\right]\delta\rho(r)dr = 0 \tag{3.35}$$

Now, as stated by Kohn and Sham' theory, the terms in the bracket in the above equation can be described by one-dimensional Schrodinger for non-interacting reference system as follows:

$$\left[\left(-\frac{1}{2}\nabla^2\right) + V_{\text{KS}}\right]\psi_i = \varepsilon_i\psi_i \tag{3.36}$$

where, $V_{\text{KS}} = J^H(r) + V_{\text{ex}}(r) + V_{\text{XC}}(r)$

And,

$$\frac{\delta}{\delta\rho(r)}\left[T_s[\rho(r)]\right] = -\frac{1}{2}\nabla_i^2$$

Here,

$$J^H(r) = \int \frac{\rho(r')}{|r-r'|}dr',$$

$$V_{\text{XC}}(r) = \frac{\delta}{\delta\rho(r)}[E_{\text{XC}}[\rho(r)]]$$

$$\lambda = \varepsilon_i$$

$$\rho(r) = \sum_{i=1}^{N}|\psi_i|^2$$

Finally, the arbitrary density is taken and V_{KS} is determined. This V_{KS} is used to find out the wavefunction and ultimately, the electron density. The process is repeated unless, the V_{KS} and $\rho(r)$ is converged (Bretonnet, 2017).

Now to determine the exchange-correlation energy item E_{XC}, the approximation required. The most widely used approximations for the exchange-correlation functional are the local density approximation (LDA), the generalized gradient approximation (GGA), and hybrid functionals.

3.2.3 Local density approximation (LDA)

LDA is the most simple approximation proposed by Kohn & Sham (1965). It is suitable in the context where the density for the system remains almost uniform . According to this approxi-

mation, the exchange-correlation term is expressed as:

$$E_{\mathrm{XC}}^{\mathrm{LDA}}[\rho(r)] = \int \rho(r)\varepsilon_{\mathrm{XC}}[\rho(r)]dr \tag{3.37}$$

where $\varepsilon_{\mathrm{XC}}[\rho(r)]$ denotes the exchange-correlation energy of each electron of interacting system and $\rho(r)$ is the density of electron in that homogeneous system. Within this approximation, the exchange energy functional is calculated using Dirac (1930) approach and correlation energy employing quantum Monte-Carlo (QMC) simulations (Bretonnet, 2017).

3.2.4 Generalized gradient approximation (GGA)

LDA can account good for only a homogeneous system. However it is not applicable for inhomogeneous and thermochemistry system where as GGA can account good for thermochemistry (Bretonnet, 2017). GGA has been developed for real system, where the distribution of electrons may not be uniform. Thus, for inhomogeneous, thermochemistry and solid state system, GGA is stated by:

$$E_{XC}^{GGA}[\rho(r)] = \int f[\rho(r), \nabla\rho(r)]dr \tag{3.38}$$

where, $\nabla\rho(r)$ represent the gradient of $\rho(r)$. Moreover, exchange functional is computed employing the method provided by Becke (1988) and the methods of calculation of correlation functional are Perdew (1986), etc.

3.2.5 Hybrid functionals

The hybrid functional is the combination of both LDA and GGA approximations. The frequently used hybrid functional is the B3LYP functional (Becke, 1988). B3LYP means Becke 3-parameter Lee, Yang, and Parr, which is composed of both exchange and correlation functional. The hybrid exchange-correlation term is defined as follows:

$$E_{xc}^{hybrid} = aE_x^{HF} + (1-a)E_x^{LDA} + cE_x^{GGA-PBE} + E_c^{LDA-PBE0} \tag{3.39}$$

where A, B, and C are parameters that provide the computed energy with the best fit to molecular atomization energies. The other terms in the right hand side like; the first two terms indicate the H-F exchange energy function based on KS orbitals, third, fourth and fifth term represent the Becke 88 exchange functional, the homogenous electron gass exact correlation component in LDA and the LYP correlation functional, respectively

3.3 Basis set

The wave function corresponding to a system is constructed using molecular orbitals. A mathematical representation of molecular orbitals (MO_s) is a basis set, that is a linear combination of basis functions. The atomic orbitals often represent the basis function (Hehre et al., 1972). The molecular orbital ψ is presented in basics of basis functions ϕ_i as given below:

$$\psi_i = \sum_{j=1}^{N} c_{ij}\phi_j \tag{3.40}$$

where $c_{(ij}$, the coefficients of the MO_s expansion, Slater-type and Gaussian-type orbitals can be considered as the most prevalent orbitals.

3.3.1 Slater and Gaussian-type orbitals

The solution obtained of Hartree-Fock equations is the atomic orbital known as wave function for a single electron in an atom. The wave function is subsequently means the basis function. Currently, Slater Type Orbitals (STO) and Gaussian Type Orbitals (GTO), both are the two most widely employed basis functions.

Slater-type orbitals have been stated as:

using spherical polar coordinates

$$\psi_{nlm}^{STO}(r,\theta,\phi) = Nr^{n-1}e^{-\beta r}Y_{lm}(\theta,\phi) \tag{3.41}$$

where, N represent the normalization constant; n being principal quantum, l is angular momentum and m is a magnetic quantum number; β is orbital exponent that controls the width of orbitals.

In cartesian coordinate,

$$\psi_{nlm}^{STO}(r,\theta,\phi) = Nx^n y^l z^n e^{-\beta r}Y_{lm}(\theta,\phi) \tag{3.42}$$

The exponential term has a more significant role in STO. With an expanding number of functions, the exponential dependence assures a surprisingly quick convergence. STOs are mostly employed in semi-empirical approaches and for atomic and diatomic systems.

Gaussian-type orbitals have been defined as:

In polar coordinate,

$$\psi_{nlm}^{GTO}(r,\theta,\phi) = N_{nlm} r^{n-1} e^{-\beta r^2} Y_{lm}(\theta,\phi) \tag{3.43}$$

where, N_{nlm} denotes the normalization constant, $r^2 = x^2 + y^2 + z^2$ and l, m, n are the integral exponentials.

In cartesian coordinate,

$$\psi_{nlm}^{GTO}(x,y,z) = N x^{n_x} y^{n_y} z^{n_z} e^{-\beta r^2} \tag{3.44}$$

The GTOs functions exhibit no cusp behavior at the nucleus, that is, slope is zero when r tends to zero, whereas STOs exhibit the proper cusp behavior, and when r tends to infinity, that is, in the tail regions, GTOs fall off rapidly while STOs decay exponentially (Perdew, 1986).

3.3.1.1 Minimal and split valence basis set

The minimal basis set is such that includes the minimum functions for representating an atomic orbital of an atom . The STO-3G minimal Basis set is the simplest basis set that consists of a single function, 1s. The one basis function, 1s, is used to express the hydrogen and helium atoms; five basis functions, i.e., 1s, 2s, $2p_x$, $2p_y$, and $2p_z$, to represent atoms from Lithium to neon; and nine basis functions, i.e., 1s, 2s,$2p_x$, $2p_y$, $2p_z$ 3s,$3p_x$, $3p_y$, $3p_z$, for atoms from sodium to argon. Further, the minimum basis set can be improved by adding extra basis functions, i.e., double-zeta or triple-zeta basis sets or so on. so, double-zeta basis is obtained by adding one extra basis function to the existing one, so it has twice as many functions as the previous ones. Similarly, the triple-zeta basis is obtained by adding two to the previous set, so it has three times as many functions as the previous ones (Hehre et al., 1972).

In a split-valence basis set, core and valence electrons are described separately. Popel and his colleagues created the n-ijG and n-ijkG Gaussian basis sets. Each valence orbital in this basis set has two or more basis functions of various sizes (Binkley, Pople, & Hehre, 1980). The double-zeta split valence basis set, n-ijG is referred to as a double-zeta split valence basis set, in which core orbitals are described by a linear combination of n Gaussian-type orbitals, while valence orbitals are represented by two separate orbitals: one composed of a linear combination of i-Gaussians and the other of j-Gaussians. Similarly, in triple-zeta split valence basis set, n-ijkG. Some examples of the split valence basis set are 3-21G, 6-31G, 6-311G, etc. The linear combination of primitive Gaussian-type orbitals is referred to as contracted Gaussian-type orbitals (CGTOs). CGTOs can be used to describe the core electrons, which reduces the computational cost (Hohenberg & Kohn, 1964).

$$\psi_{nlm}^{CGTO}(x,y,z) = \sum_{i=1}^{n} c_i x^l y^m z^n e^{-\beta r^2} \tag{3.45}$$

3.3.2 Polarization and diffuse function

For anisotropic charge distribution, only increasing the basis set to double or triple or higher-zeta basis set may not improve the result. However, the result can be promoted by adding the orbital of greater momentum compared to the adjusted one, known as the polarized basis. For example, basis function p can be added to s occupied orbital and d can be added to p orbital, so that the occupied orbitals are polarized. The examples of polarized basis sets are 6-311G*/6-311G(d),6-311G**/ 6-311G(d,p), etc. Here, 6-311G* represents that polarized function has been added to the heavy atoms and 6-311** represents that polarized function has been added to both hydrogen as well as heavy atoms.

Moreover, for the system which may characterize with either of the properties like as, lone pair, anions, a lot of negative charge or low ionization potentials, the result can be improved using diffuse functions. The diffuse function is the additional s and p-type orbitals to the atoms. The examples of diffuse functions are 6-31+, 6-31++ etc.Here, 6-31+ denotes the addition of a diffuse function for heavy atoms, while 6-31++ indicates the inclusion of diffuse functions for both hydrogen and heavy atoms (Krishnan, Binkley, Seeger, & Pople, 1980)).

3.4 Used Materials

3.4.1 Gaussian 16W

Gaussian 16W is the latest version of the Gaussian program, a sophisticated computational chemistry software tool used to model, simulate, and conduct various quantum chemical calculations of atoms, molecules, and other reactive systems. John Pople and his colleagues at Carnegie Mellon University initially released this software under the name Gaussian 70 in 1970 (Frisch et al., 2009). Due to this significant development, which has made substantial contributions to the field, Pople was decorated with the Nobel Prize in the field of Chemistry in 1998 for his contributions in developing computational methods in quantum chemistry (Salahub et al., 1991). Since its release, Gaussian has been revised and updated multiple times and has become widely popular and useful among chemists, chemical engineers, physicists, biochemists, and other researchers due to its increasing credibility, reliability, cost-efficiency, and time-efficiency features. This versatile software offers advanced capabilities for predicting energies, structures, vibrational frequencies, transition states, and various other significant properties of chemical systems based on ab initio calculations, including Hartree-Fock (HF) & Post-Hartree-Fock methods, Density Functional Theory (DFT), semi-empirical methods, molecular dynamics, and other hybrid methods (Frisch et al., 2009). Furthermore, It is capable of generating theoretical spectra, including UV-Vis, IR, and NMR, that could be directly leveled with experimental data. This feature is highly valuable for analyzing experimental outcomes and confirming the accuracy of computational models.

3.4.2 GaussView 6

GaussView 6 is the Graphical User Interface (GUI) for Gaussian, with the number six indicating its latest edition. It allows users to observe molecules from all possible angles in 3D, enabling zooming, rotating, and even altering the bond lengths, angles between various bonds of various atoms within the molecules. It generates Gaussian files of the molecules or atoms, which serve as input files to execute optimization and desired calculations based on various principles within Gaussian. It facilitates easy visualization of the results and allows for more detailed analysis by displaying molecular orbitals, electrostatic molecular potential, electron density maps, vibrational modes, and other properties. Additionally, it includes features for visualizing different spectra and interpreting them. This latest version offers enhanced visualization and supports more complex molecular systems.

3.4.3 GaussSum 3.0

GaussSum 3.0 is a graphical user interface (GUI) and post-processing tool in computational chemistry, capable of analyzing and visualizing the output of electronic structure calculations conducted using Gaussian. It can be used to analyze spectra, such as UV-Vis absorption spectra

and IR spectra, visualize molecular orbitals, and handle data from Gaussian results. It is robust software for analyzing theoretical calculation data from Gaussian.

3.4.4 SwissADME and ProTox-3.0

For a compound to be an applicable medicine, it should exhibit high biological interaction, minimal toxicity, and be able to reach and maintain an appropriate concentration at the therapeutic target in the body. Considering all these factors, an ADME study is crucial in the development of novel lead compounds (Tetko et al., 2006). A molecules pharmacokinetic properties are addressed in ADME studies, covering absorption, distribution, metabolism, and excretion; these are crucial elements in contemporary drug development. The applications of *in silico* methods via online platforms upgrades ADME investigation much easier in today's context (Balani et al., 2005).

SwissADME is a tool based on the web developed and regulated by the molecular modeling group belonging to the Swiss Institute of Bioinformatics (SIB), available free of charge at [http://www.swissadme.ch] (Daina, Michielin, & Zoete, 2017). It enables the prediction of ADME parameters, pharmacokinetics, drug-likeness, and medicinal chemistry suitability, along with the computation of physicochemical descriptors for small molecules in drug discovery. According to the official site, the main motive behind SwissADME is to provide open availability to a number of parameters and anticipatory algorithms to compute & estimate the druglikeness of small molecules (Daina et al., 2017). SwissADME's accessibility allows researchers of all levels to utilize it for their studies. Extra care should be exercised if the platform is employed for non-drug-related activities.

ProTox-3.0 is also a web-based tool and it is builted by the Computational Toxicology Group at the Charité University Hospital in Berlin, Germany (Banerjee, Kemmler, Dunkel, & Preissner, 2024). The full form of ProTox is "Prediction of Toxicity". It integrates various modern and advanced algorithms to estimate and forecast toxicity endpoints, taking account of acute toxicity, hepatotoxicity, cytotoxicity, carcinogenicity, mutagenicity, immunotoxicity, adverse outcome pathways (Tox21), and toxicity targets. It provides a free, no-login-required web server for *in-silico* toxicity projection and estimation at https://tox.charite.de/proTox-3.0 (Drwal, Banerjee, Dunkel, Wettig, & Preissner, 2014). Users can input two-dimensional chemical structures and receive a toxicity logs for thirty-three models, along with confidence marks and a comprehensive radar chart for toxicity.

3.4.5 Jupyter Notebook

Jupyter Notebook is an interactive browser-based tool that is very useful for writing and displaying code, showing the outputs generated by the code, and adding commentary about the code. It supports multiple programming languages, but Python is preferred by most users. It

is a very useful tool in STEM fields for analyzing data, performing computations, and presenting results in a well-organized and clear manner. In our research, it is used to plot spectra graphs, which consist of a large number of coordinates and would be too time-consuming to do manually.

3.5 Methods

3.5.1 DFT calculations

Initially, the 3D structure files for allicin and trigonelline were first retrieved in SDF format from the PubChem website and then imported into GaussView 6 software. After that, by using the GaussView 06 Software, the Gaussian input files for Allicin and Trigonelline were generated. These molecules were then optimized, followed by quantum chemical calculations using the DFT method at the Becke 3-parameter, Lee-Yang-Parr (B3LYP)/6-311++G(d,p) level of calculation, by employing Gaussian 16W software. Negative frequencies were eliminated by reoptimizing the molecules. Different molecular characteristics namely; Dipole moment, Mulliken charges, Molecular electrostatic potential (MEP), Highest occupied molecular orbital (HOMO), Lowest unoccupied molecular orbital (LUMO), and optimized parameters, were computed. For spectral analysis, UV-Vis spectra was produced implementing the time-dependent (TD)-DFT method at the same level of calculation. Throughout the work, GaussView 6 and GaussSum 3.0 were employed for visualization and further detailed analysis, while Jupyter Notebook was used for plotting graphs manually with the produced coordinates.

3.5.2 Drug likeliness and Toxicity prediction

The absorption, distribution, metabolism, excretion, and toxicity (ADMET) of these molecules were computed with the help the SwissADME and ProTox-3.0 websites by entering the canonical SMILES of these molecules taken from the PubChem website [https://pubchem.ncbi.nlm.nih.gov/]. These calculations helped evaluate their physicochemical, lipophilic, pharmacokinetic, medicinal chemistry friendliness and drug-likeness parameters, along with their potential harmfulness to the human body.

CHAPTER 4

4. RESULTS AND DISCUSSION

4.1 Geometry optimization and stability analysis

Allicin and Trigonelline were optimized using the 6-311++G(d,p) basis set at the B3LYP level of approximation, and the optimized molecular conformation of these molecules with atomic numbering in a neutral state is presented in Figure 3.

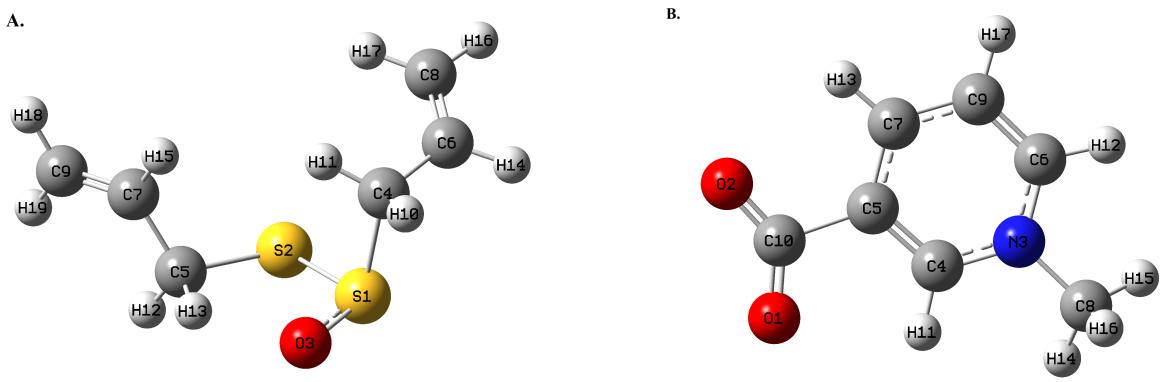

Figure 3: Optimized structure and numbering for (A) Allicin and (B) Trigonelline.

The optimized parameters i.e bond angles, bond length and Tetrahedral angle of allicin and trigonelline from their optimized structures are tabulated below in Table 1 and 2, respectively. In Allicin, there are five types of bonds in the optimized structure: S–S, S–O, S–C, C=C, and C–H. The bond between sulfur and oxygen is a coordinate covalent bond where sulfur donates its lone pairs of electrons to oxygen ($S \rightarrow O$). There are two double coordinate covalent bonds between carbon atoms, while all other bonds are single covalent bonds. The results of the calculations show that the longest bond in the system is the S(1)–S(2) bond, which is 2.2358 Å, and the shortest bond is the C(8)–H(16) bond at 1.0838 Å. The highest bond angle corresponds to C(5)–C(7)–C(9), and the highest dihedral angle corresponds to H(14)–C(6)–C(8)–H(17). The lowest bond angle and dihedral angle correspond to S(1)–S(2)–C(5) and C(4)–C(6)–C(8)–H(17), respectively.

In trigonelline, there are four types of bonds in the optimized structure: C–O, N–C, C–C, and C–H. Among these bonds, there are four coordinate covalent bonds, four double covalent bonds, and the rest are single covalent bonds. The results of the calculations show that the longest bond in the system is the C(5)=C(10) bond, which is 1.5669 Å, and the shortest bond is the C(6)–H(12) bond at 1.0811 Å. The highest bond angle corresponds to O(1)–C(10)–O(2), and the highest dihedral angle corresponds to C(4)–C(5)–C(7)–H(13). The lowest bond angle and dihedral angle correspond to N(3)–C(8)–H(14) and C(4)–N(3)–C(6)–C(9), respectively.

Table 1: Optimized parameters of the Allicin.

Bond	Bond Length (Å)	Bond Angle	Bond Angle Value (°)	Dihedral Angle	Diahedral Angle Value (°)
S(1)-S(2)	2.2358	S(2)-S(1)-O(3)	107.1004	O(3)-S(1)-S(2)-C(5)	11.8059
S(1)-O(3)	1.5081	S(2)-S(1)-C(4)	99.1966	C(4)-S(1)-S(2)-C(5)	-97
S(1)-C(4)	1.8814	O(3)-S(1)-C(4)	104.9014	S(2)-S(1)-C(4)-C(6)	-76.1267
S(2)-C(5)	1.8459	S(1)-S(2)-C(5)	97.9715	S(2)-S(1)-C(4)-H(10)	163.5385
C(4)-C(6)	1.4899	S(1)-C(4)-C(6)	111.8565	S(2)-S(1)-C(4)-H(11)	48.4887
C(4)-H(10)	1.0932	S(1)-C(4)-H(10)	101.8166	O(3)-S(1)-C(4)-C(6)	173.3048
C(4)-H(11)	1.0891	S(1)-C(4)-H(11)	106.6849	O(3)-S(1)-C(4)-H(10)	52.97
C(5)-C(7)	1.4951	C(6)-C(4)-H(10)	112.4935	O(3)-S(1)-C(4)-H(11)	-62.0797
C(5)-H(12)	1.0908	C(6)-C(4)-H(11)	113.4626	S(1)-C(5)-C(7)-C(9)	110.5418
C(5)-H(13)	1.0995	H(10)-C(4)-H(11)	109.7666	S(1)-C(5)-C(7)-H(15)	-126.3868
C(6)-C(8)	1.3325	S(2)-C(5)-C(7)	113.2703	S(1)-C(5)-C(7)-H(13)	-11.8078
C(6)-H(14)	1.0873	S(2)-C(5)-H(12)	106.2698	S(1)-C(4)-C(6)-C(8)	106.7359
C(7)-C(9)	1.3315	S(2)-C(5)-H(13)	105.2648	S(1)-C(4)-C(6)-H(14)	-72.3288
C(7)-H(15)	1.0874	C(7)-C(5)-H(12)	111.7487	H(10)-C(4)-C(6)-C(8)	-139.3791
C(8)-H(16)	1.0838	C(7)-C(5)-H(13)	111.7279	H(10)-C(4)-C(6)-H(14)	41.5562
C(8)-H(17)	1.0847	H(12)-C(5)-H(13)	108.1461	H(11)-C(4)-C(6)-C(8)	-14.0162
C(9)-H(18)	1.0838	C(4)-C(6)-C(8)	124.2136	H(11)-C(4)-C(6)-H(14)	166.9191
C(9)-H(19)	1.0858	C(4)-C(6)-H(14)	116.3564	S(2)-C(5)-C(7)-C(9)	115.3243
		C(8)-C(6)-H(14)	119.4235	S(2)-C(5)-C(7)-H(15)	-65.464
		C(5)-C(7)-C(9)	124.313	H(12)-C(5)-C(7)-C(9)	-4.6694
		C(5)-C(7)-H(15)	116.1254	H(12)-C(5)-C(7)-H(15)	174.5424
		C(9)-C(7)-H(15)	119.5569	H(13)-C(5)-C(7)-C(9)	-125.9972
		C(6)-C(8)-H(16)	121.2919	H(13)-C(5)-C(7)-H(15)	53.2146
		C(6)-C(8)-H(17)	121.6951	C(4)-C(6)-C(8)-H(16)	-179.6359
		H(16)-C(8)-H(17)	117.013	C(4)-C(6)-C(8)-H(17)	0.4429
		C(7)-C(9)-H(18)	121.545	H(14)-C(6)-C(8)-H(16)	-0.5981
		C(7)-C(9)-H(19)	121.6023	H(14)-C(6)-C(8)-H(17)	179.4807
		H(18)-C(9)-H(19)	116.8519	C(5)-C(7)-C(9)-H(18)	178.7259
				C(5)-C(7)-C(9)-H(19)	-0.9367
				H(15)-C(7)-C(9)-H(18)	-0.4605
				H(15)-C(7)-C(9)-H(19)	179.8768

Table 2: Optimized parameters of the Trigonelline.

Bond	Bond Length (Å)	Bond Angle	Bond Angle Value (°)	Dihedral Angle	Diahedral Angle Value (°)
O(1) - C(10)	1.245	C(4) - N(3) - C(6)	120.6725	C(6) - N(3) - C(4) - C(5)	-0.0853
O(2) - C(10)	1.239	C(4) - N(3) - C(8)	119.6374	C(6) - N(3) - C(4) - H(11)	179.7969
N(3) - C(4)	1.3532	C(6) - N(3) - C(8)	119.651	C(8) - N(3) - C(4) - C(5)	177.633
N(3) - C(6)	1.3575	N(3) - C(4) - C(5)	121.5058	C(8) - N(3) - C(4) - H(11)	-2.4848
N(3) - C(8)	1.477	N(3) - C(4) - H(11)	118.9172	C(4) - N(3) - C(6) - C(9)	-0.0118
C(4) - C(5)	1.3839	C(5) - C(4) - H(11)	119.5768	C(4) - N(3) - C(6) - H(12)	-179.9509
C(4) - H(11)	1.0836	C(4) - C(5) - C(7)	118.2383	C(8) - N(3) - C(6) - C(9)	-177.7298
C(5) - C(7)	1.3923	C(4) - C(5) - C(10)	118.874	C(8) - N(3) - C(6) - H(12)	2.3311
C(5) - C(10)	1.5669	C(7) - C(5) - C(10)	122.8876	C(4) - N(3) - C(8) - H(14)	29.1223
C(6) - C(9)	1.379	N(3) - C(6) - C(9)	120.2772	C(4) - N(3) - C(8) - H(15)	148.6836
C(6) - H(12)	1.0811	N(3) - C(6) - H(12)	116.4228	C(4) - N(3) - C(8) - H(16)	-90.7876
C(7) - C(9)	1.3979	C(9) - C(6) - H(12)	123.2999	C(6) - N(3) - C(8) - H(14)	-153.1358
C(7) - H(13)	1.0848	C(5) - C(7) - C(9)	119.8685	C(6) - N(3) - C(8) - H(15)	-33.5746
C(8) - H(14)	1.0877	C(5) - C(7) - H(13)	117.4889	C(6) - N(3) - C(8) - H(16)	86.9542
C(8) - H(15)	1.0886	C(9) - C(7) - H(13)	122.6424	N(3) - C(4) - C(5) - C(7)	0.033
C(8) - H(16)	1.091	N(3) - C(8) - H(14)	108.9159	N(3) - C(4) - C(5) - C(10)	179.9277
C(9) - H(17)	1.0828	N(3) - C(8) - H(15)	109.4185	H(11) - C(4) - C(5) - C(7)	-179.8485
		N(3) - C(8) - H(16)	109.6833	H(11) - C(4) - C(5) - C(10)	0.0463
		H(14) - C(8) - H(15)	109.4135	C(4) - C(5) - C(7) - C(9)	0.1129
		H(14) - C(8) - H(16)	109.5698	C(4) - C(5) - C(7) - H(13)	179.9804
		H(15) - C(8) - H(16)	109.8221	C(10) - C(5) - C(7) - C(9)	-179.7774
		C(6) - C(9) - C(7)	119.4373	C(10) - C(5) - C(7) - H(13)	0.0901
		C(6) - C(9) - H(17)	118.8525	C(4) - C(5) - C(10) - O(1)	-0.7668
		C(7) - C(9) - H(17)	121.71	C(4) - C(5) - C(10) - O(2)	179.2032
		O(1) - C(10) - O(2)	133.6283	C(7) - C(5) - C(10) - O(1)	179.1228
		O(1) - C(10) - C(5)	112.9129	C(7) - C(5) - C(10) - O(2)	-0.9072
		O(2) - C(10) - C(5)	113.4589	N(3) - C(6) - C(9) - C(7)	0.1569
				N(3) - C(6) - C(9) - H(17)	-179.7113
				H(12) - C(6) - C(9) - C(7)	-179.9083
				H(12) - C(6) - C(9) - H(17)	0.2235
				C(5) - C(7) - C(9) - C(6)	-0.2071
				C(5) - C(7) - C(9) - H(17)	179.6572
				H(13) - C(7) - C(9) - C(6)	179.9325
				H(13) - C(7) - C(9) - H(17)	-0.2033

The geometrical parameters were calculated that includes total energy (global minimum energy), dipole moment, the RMS Cartesian force and the maximum Cartesian force of the molecules are shown in Table 3.

The smaller values of the root mean square (RMS) Cartesian force and maximum Cartesian force relects that the compounds under study have gained their stable geometries and conformation (Kudin & Scuseria, 2000). The total energy(Global Minimunm energy) for Allicin (-1106.3181 Hartrees) is relatively lower than Trigonelline (-476.26062 Hartrees) which signifies that Allicin has more stabilty than Trigonelline. Unstable drug molecules may have low bioavailability, a short shelf life, and may not maintain their intended structure and function over time, leading to inconsistent efficacy and potential safety issues as they decompose into byproducts and lose their therapeutic effects (Snape, Astles, & Davies, 2010; Haneef, Amir, Sheikh, & Chadha, 2023). Comparing the stability based on global minimum energy, Allicin could be a comparatively better potential drug candidate than Trigonelline.

The dipole moment reveals the distribution of charges within a molecule, offering insight into how charge moves throughout its structure (Noureddine, Issaoui, & Al-Dossary, 2021). The computed value of the dipole moment for Allicin is 2.7117 Debye while for Trigonelline is 14.4698 Debye, respectively. The huge difference in dipole moments of two molecules suggests stronger intermolecular interaction of Trigonelline compounds promoting the formation of number of hydrogen bonds than that of Allicin (Issaoui, Ghalla, Muthu, Flakus, & Oujia, 2015). Molecules with higher dipole values enhance solubility and bioavailability but may reduce permeability; both are essential for a chemical to be a drug, so the appropriate dipole value should be chosen based on the specific use case (Pereira & Aires-de Sousa, 2018).

Allicin and Trigonelline can participate in interaction with proteins via dipole-dipole interactions, impacting the binding energy of the system, which can be affected by the dipole. (Lien, Guo, Li, & Su, 1982).

Table 3: Calculated total energy, dipole moment, RMS cartesian force, and maximum cartesian force of Allicin and Trigonelline.

Molecules	Total energy (E)	Dipole moment (μ)	RMS cartesian force (Hartrees/Bohr)	Maximum cartesian Force (Hartrees/Bohr)
Allicin	-1106.3181	2.7117	6.74×10^{-7}	1.809×10^{-6}
Trigonelline	-476.26062	14.4698	1.474×10^{-6}	8.738×10^{-6}

4.2 Molecular electrostatic potential

MEP maps are helpful to interpret the reactive properties of molecules related to electrophilic and nucleophilic attacks and intermolecular interactions (Demircioğlu, Kaştaş, & Büyükgüngör, 2015). The reactive electrophilic sites and reactive nucleophilic sites: both helps in the forma-

tion of hydrogen bonds (Taghour et al., 2022). The corresponding MEP maps along with contour lines for Allicin and Trigonelline is shown in the figure 4 and 5 respectively. Molecullar electrostatic potential diagram displays diffrent level of electrostatic potential regions through color labelling. The color coding of MEP map illustrates the electrostatic potential, with red indicating the highest potential regions with strong attraction, followed by yellow, green, and blue for progressively lower potentials with strong repulsion. For Allicin, the potential ranges from -0.88 a.u. (red) to 0.88 a.u. (blue), while for Trigonelline, it ranges from -0.16 a.u. (red) to 0.16 a.u. (blue). Yellow and green represent neither more postive nor more negative levels of electrostatic potential i.e they represents almost neutral level.

The oxygen atom O3 in Allicin shows the most negative charges while O1 and O2 in Trigonelline have the maximum negative charges, denoting nucleophilic sites. The most positive areas are situated around the vicinity of the hydrogen atoms H10, H14, and H17 in Allicin, and H12, H15, H16, and H17 in Trigonelline, signifying potential sites for electrophilic attack. Additionally, both sulfur atoms in Allicin have considerable negative potential regions in their surroundings. Therefore, these sites has significant role in the biological activities of the molecule and process of formation of intermolecular hydrogen bonds within crystal packing (Lien et al., 1982).

Additionally, both positive and negative potential regions are evident in the vicinity of the carbon atoms in each of the molecules, reflecting a complex distribution of electrostatic potential in these areas.

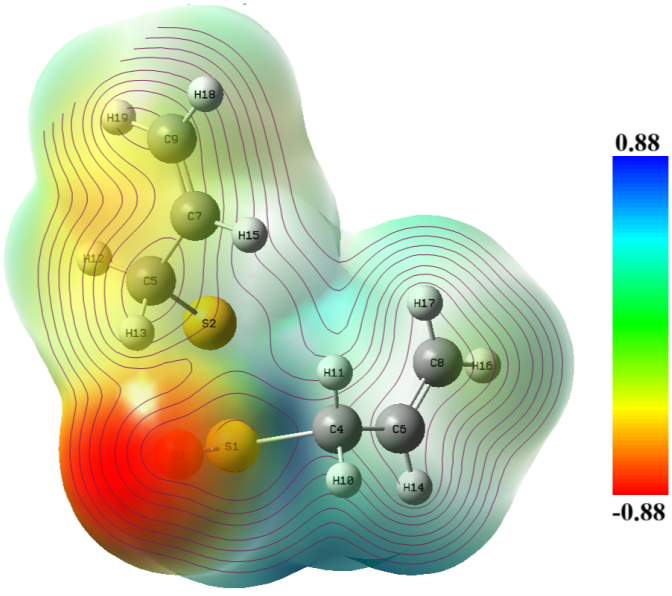

Figure 4: Molecular electrostatic potential map with contour lines for Allicin.

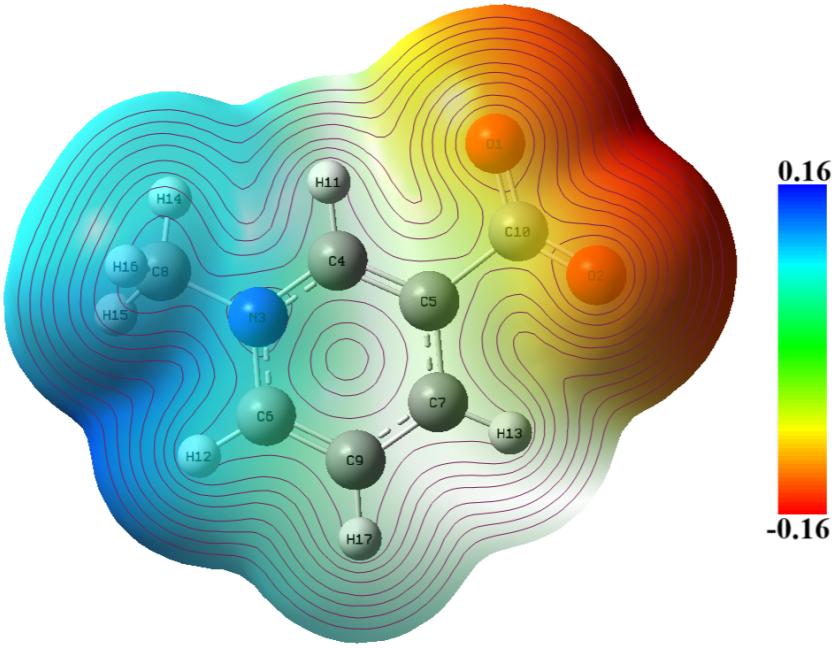

Figure 5: Molecular electrostatic potential map with contour lines for Trigonelline.

4.3 Mulliken atomic charges

Mulliken atomic charges, which estimate the partial charges on the atoms within the molecule, are valuable to understand how molecules react, particularly in terms of electrophilic and nucleophilic attacks (Demircioğlu et al., 2015). This approach is commonly applied in quantum chemical calculations due to its importance in determining a molecule's polarizability, electronic structure, dipole moment, and other critical properties (Taghour et al., 2022). The Mulliken atomic charge distributions for Allicin and Trigonelline are presented in Table 4. The comparative bar graph for mulliken charges of both compound is shown in the Figure 6.

For Allicin, Mulliken charges indicate that oxygen atoms carry negative charges, while hydrogen atoms are positively charged. Sulfur and carbon atoms show both negative and positive charges. In Trigonelline, oxygen atoms also bear negative charges, but nitrogen and hydrogen atoms are positively charged, with carbon atoms exhibiting a mix of negative and positive charges.

Mulliken charge with the highest positive value has great importance. In Allicin, this value is found on sulfur atom S1 and in Trigonelline it is found in carbon atom C5. Conversely, the smallest negative charges are presented in the carbon atoms C4 in Allicin and C10 in Trigonelline. Among hydrogen atoms, the majority of the Mulliken charge is concentratd in hydrogen atom H10 in Allicin and on H13 in Trigonelline.

These charge distributions highlight the polar nature of both Allicin and Trigonelline molecules. The presence of electrophilic and nucleophilic sites makes them potentially reactive with other biological molecules, which may impact their interactions and biological activity in the human body. Such detailed charge analysis can help predict their behavior in biochemical pathways and assess their potential therapeutic effects (Taghour et al., 2022).

Table 4: Mulliken atomic charges for Allicin and Trigonelline.

Allicin		**Trigonelline**	
Atom	**Charge**	**Atom**	**Charge**
S1	0.488464	O1	-0.429286
S2	-0.148803	O2	-0.403156
O3	-0.433046	N3	0.228406
C4	-0.557744	C4	-0.454513
C5	-0.512805	C5	0.562004
C6	0.187149	C6	-0.108680
C7	0.209507	C7	0.327271
C8	-0.461630	C8	-0.319916
C9	-0.476818	C9	-0.387145
H10	0.249467	C10	-0.513691
H11	0.238051	H11	0.253450
H12	0.158217	H12	0.183022
H13	0.200581	H13	0.271465
H14	0.165550	H14	0.185832
H15	0.165957	H15	0.159585
H16	0.134143	H16	0.226715
H17	0.123367	H17	0.218638
H18	0.137185		
H19	0.133208		

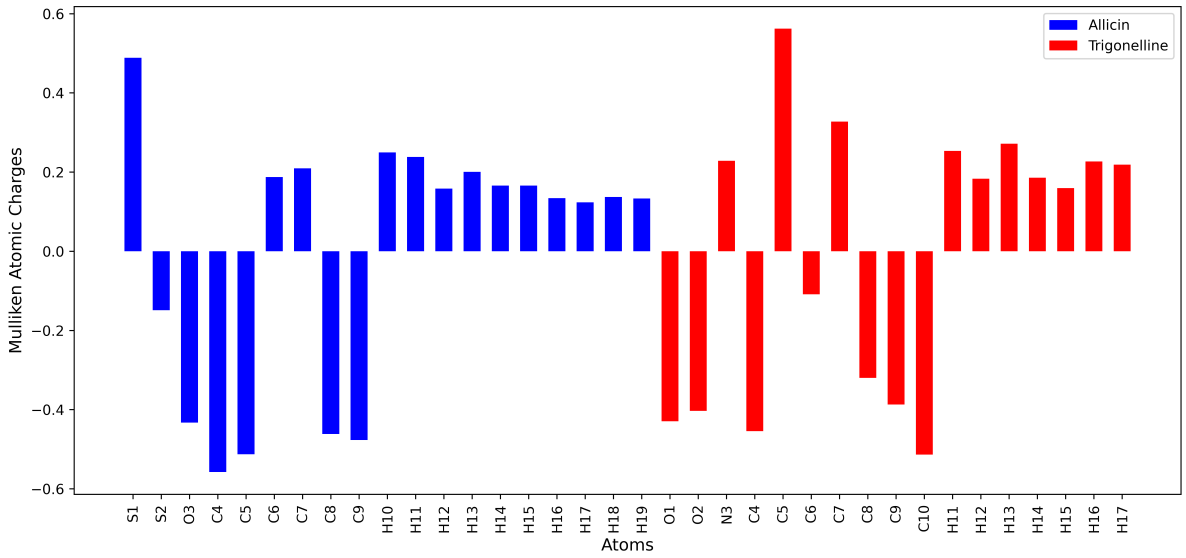

Figure 6: Mulliken atomic charge distributions of Allicin and Trigonelline.

4.4 Frontier molecular orbitals

Electronic absorption (UV-Vis) spectra for these two compounds were calculated using the TD-DFT method at the B3LYP/6-311++G(d,p) level, as shown in Figures 7 and 8. For Allicin, the wavelengths 265.75 nm and 389.6 nm correspond to its electronic transitions. Notably, the transition with the highest oscillatory strength occurs at 289 nm, attributed to the transition from the electron donating orbital (HOMO) to the electron accepting orbital (LUMO), as detailed in Table 5. Trigonelline, on the other hand, shows a wavelength of 527.9 nm, with the maximum oscillatory strength observed at 528 nm, which is associated with the transition from HOMO-2 to LUMO.

Table 5: Calculated electronic properties of Allicin and Trigonelline.

Compound	Wavelength (nm)	Oscillatory strength	Contributions
Allicin	340	0.0071	HOMO → LUMO (95%)
	289	0.008	HOMO-1 → LUMO (91%) HOMO-4 → LUMO (3%) HOMO-3 → LUMO (2%)
	262	0.02	HOMO → LUMO+1 (87%) HOMO → LUMO+2 (8%)
Trigonelline	642	0.0	HOMO → LUMO (99%)
	637	0.0	HOMO-1 → LUMO (98%)
	528	0.0162	HOMO-2 → LUMO (99%)

The frontier molecular orbitals (FMOs) are employed to predict reactivity. In these orbitals, the green regions around the atoms represent negative charge phases and red regions around the atoms represent positive charge phases (Barım & Akman, 2019). This visualization provides a clear depiction about charge distribution within the molecule (Mishra, Joshi, Srivastava,

Tandon, & Jain, 2014).

The key molecular orbitals participating in chemical reactivity and the stability of the compounds are the HOMO (Highest Occupied Molecular Orbital) and LUMO (Lowest Unoccupied Molecular Orbital). The energy of the HOMO (E_{H}) and the LUMO (E_{L}), along with their energy gap ($\Delta E_{\mathrm{L\text{-}H}}$), are indicative of the molecule's biological activity (Atkins, 2001). The HOMO and LUMO orbitals, which relate to ionization potential and electron affinity respectively, describe the molecule's ability to donate and accept electrons (Borah & Devi, 2020). Figure9 and figure10 show the HOMO and LUMO energy and their gap for Allicin and Trigonelline respectively. The computed LUMO value of Allicin is -1.85 eV, while for Trigonelline it is -3.05 eV, indicating that Allicin has a higher electron affinity compared to Trigonelline. The energy differences, calculated as the subtraction of E_{HOMO} from E_{LUMO}, are 4.46 eV for Allicin and 2.76 eV for Trigonelline. A smaller energy gap facilitates electron flow, making Trigonelline more reactive and softer than Allicin. The compound having a high HOMO energy acts as an effective electron donor, whereas the compound having a low LUMO energy serves as an efficient electron acceptor (Kumar, Vasudevan, Prakasam, Geetha, & Anbarasan, 2010). Therefore, Trigonelline is a more effective electron donor compared to Allicin due to its higher HOMO energy. Overall, these findings suggest that both Allicin and Trigonelline are capable of facilitating charge transfer and possess significant potential for biological activities (Fouad & Adly, 2021).

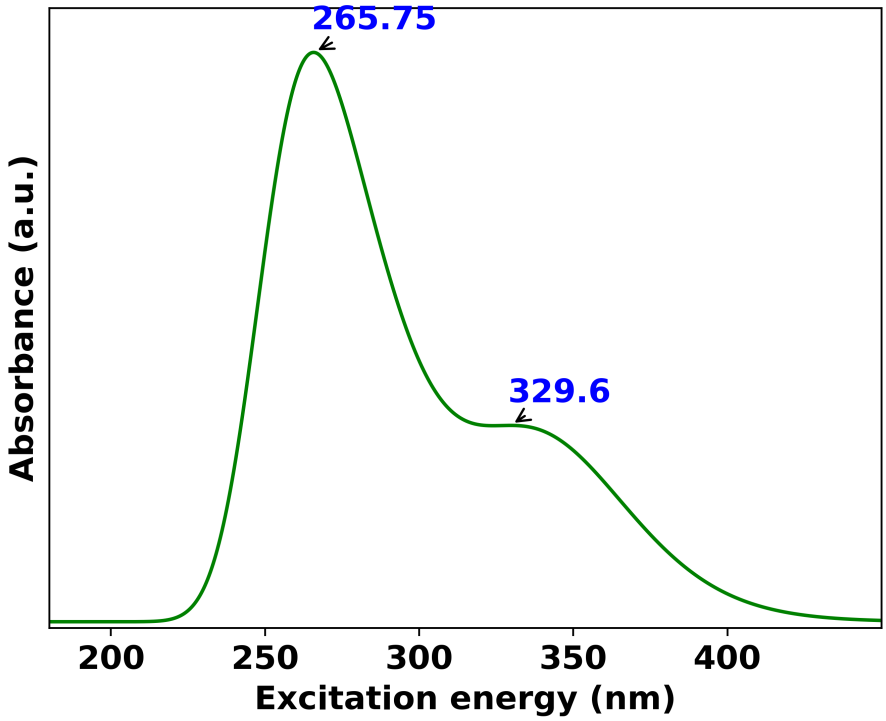

Figure 7: UV-Vis absorption spectrum of Allicin.

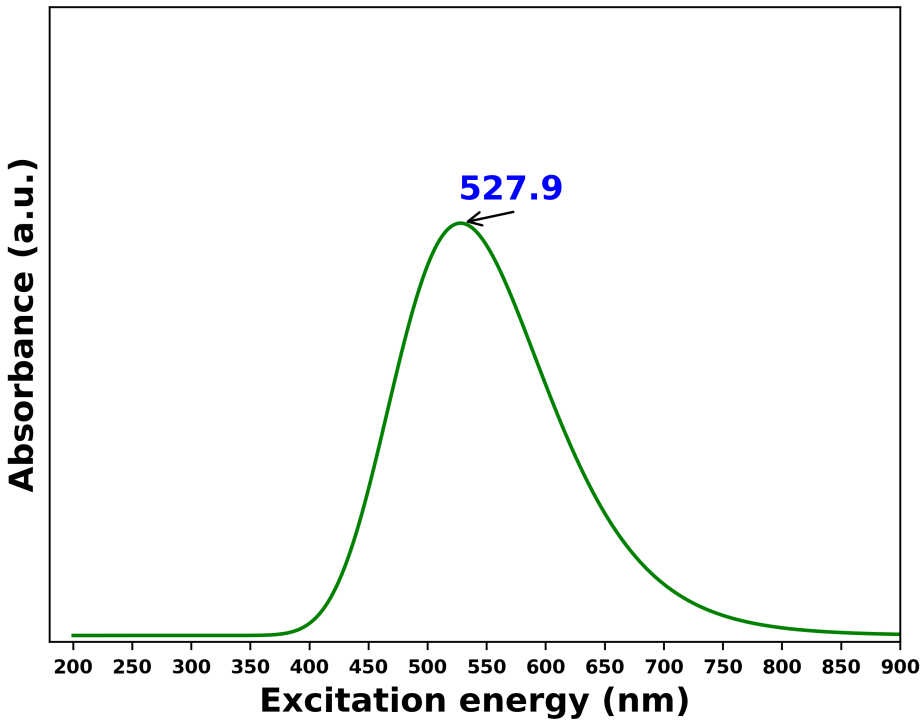

Figure 8: UV-Vis absorption spectrum of Trigonelline.

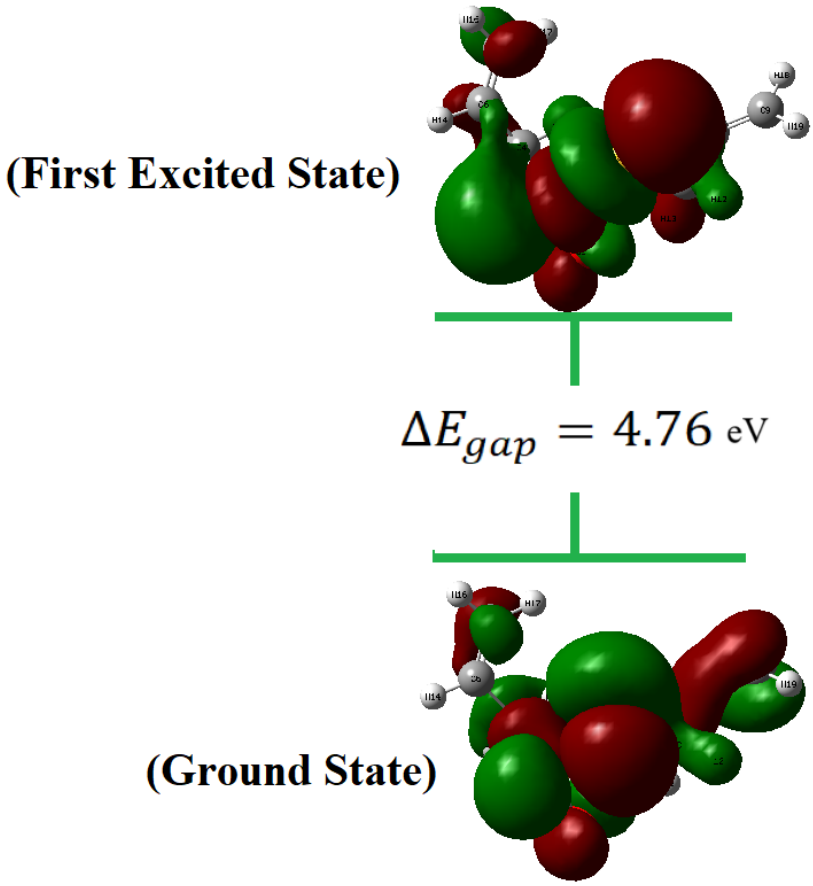

Figure 9: Energy gap between HOMO and LUMO in Allicin.

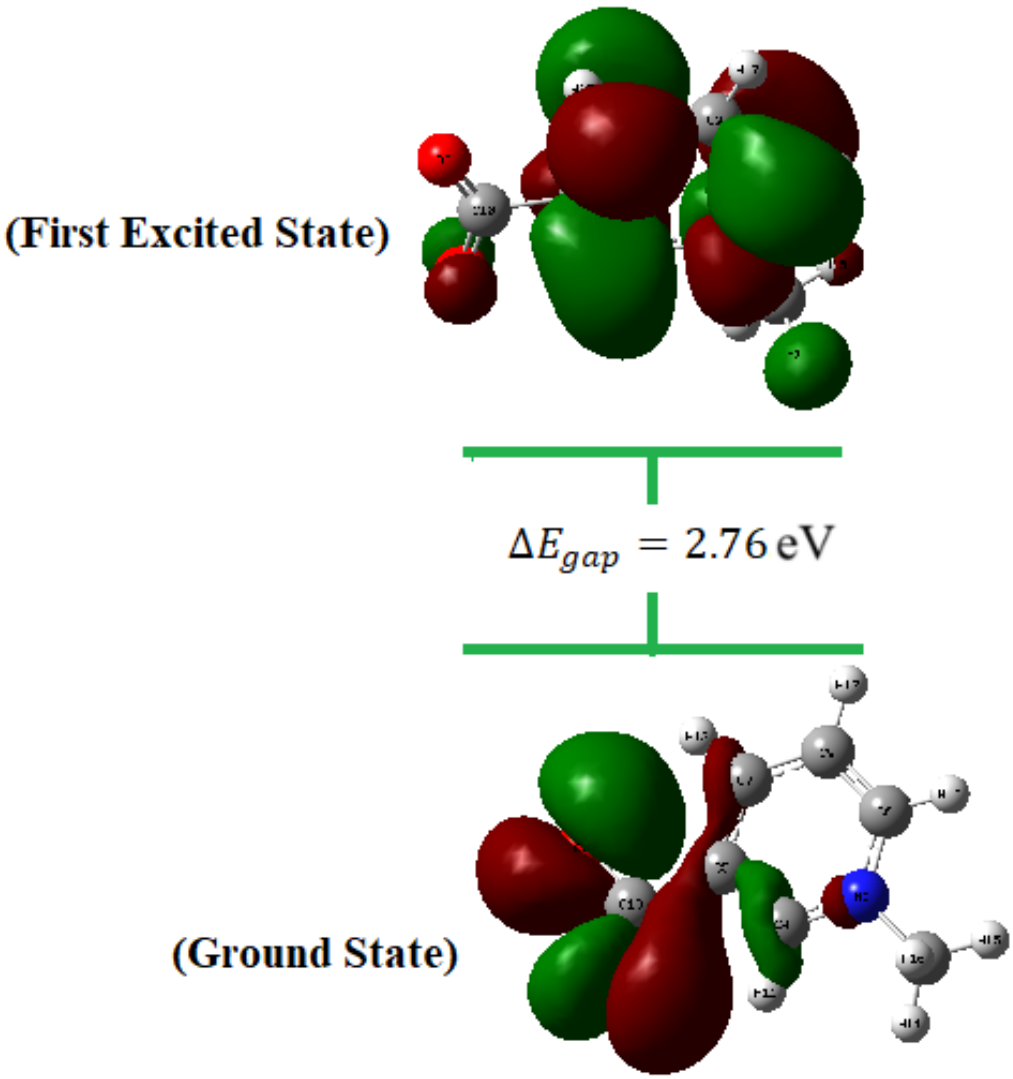

Figure 10: Energy gap between HOMO and LUMO in Trigonelline.

4.5 Global reactivity descriptors:

Using Koopmans' principles, the ionization potential ($I = -E_{\text{HOMO}}$) and electron affinity ($A = -E_{\text{LUMO}}$) for Allicin and Trigoneline were determined (Pearson, 1988). These calculations allow for the prediction of global reactive descriptors, including chemical hardness ($\eta = \frac{I-A}{2}$), chemical softness ($S = \frac{1}{\eta}$), electronic chemical potential ($\mu = -\frac{I+A}{2}$), and the global electrophilicity index ($\omega = \frac{\mu^2}{2\eta}$) (Pearson, 1988). Table 6 shows the calculated values of global reactivity descriptors of both compounds.

Table 6: Global reactivity descriptors for Allicin and Trigonelline.

Parameter	**Allicin**	**Trigonelline**
HOMO	-6.61 eV	-5.81 eV
LUMO	-1.85 eV	-3.05 eV
$E_{\text{LUMO}} - E_{\text{HOMO}}$	4.76 eV	2.76 eV
Ionization Potential Energy (I)	6.61 eV	5.81 eV
Electron Affinity (A)	1.85 eV	3.05 eV
Electronegativity (χ)	4.23 eV	4.43 eV
Electronic Chemical Potential (μ)	-4.23 eV	-4.43 eV
Chemical Hardness (η)	2.38 eV	1.38 eV
Chemical Softness (S)	0.42 $(\text{eV})^{-1}$	0.72 $(\text{eV})^{-1}$
Global Electrophilicity Index (ω)	3.76 eV	7.11 eV

Allicin and Trigonelline exhibit non-negative values for both chemical hardness and Global electrophilicity index (Parr, Szentpály, & Liu, 1999). Positive values of this both parameter signifies that both molecfules are conducive to charge exchange processes within the molecules and may influence binding affinity in the interactions between receptor and ligand (Parr et al, 1999). The chemical hardness (η) reflects the capacity for charge transfer within the molecules (Padmanabhan, Parthasarathi, Subramanian, & Chattaraj, 2007).

Morever, the chemical softness (S) of Allicin (0.72 eV) is found to be lower compared to Trigonelline (0.42 eV), suggesting that Trigonelline is more reactive than Allicin (Fouad & Adly, 2021). Molecules with lower Ionization potential (IP) values can more readily donate electrons to neutralize free radicals (Tayyem & Almatarneh, 2016). Considering this fact, Trigonelline has a lower ionization potential energy than allicin, indicating that it has comparatively better antioxidant properties than Allicin.

The difference energy in the HOMO and LUMO for Allicin and Trigonelline are found to be 4.76 eV and 2.76 eV, sequentially. The small values values symbolizes small energy gaps, which indicate that the molecules are chemically reactive, with Trigonelline being more reactive, and both can participate in interactions of transferring charge within the molecules (Gunasekaran, Balaji, Kumeresan, Anand, & Srinivasan, 2008). The calculated Global electrophilicity index , 3.76 eV for Allicin and 7.11 eV for Trigonelline taking together their

electronic chemical potentials, indicate the avaibility of prominent electrophilic characteristics within these two molecules. Also this computed electrophilicity offers perception about the biological activeness of Allicin and Trigonelline. Low values of electronic chemical potential (μ) i.e. -4.23 eV for Allicin and -4.43 eV for Trigonelline, relects the ability of the both molecules to donate the electrons.

4.6 Druglikeness and Toxicity:

Integrating computer-based simulations into evaluations of drug absorption, distribution, metabolism, excretion, and potential harmful effects can enhance efficiency in terms of costs, time, and resources during the drug development process (Bitew et al., 2021). Theoretical evaluation of the lipophilicity, as indicated by the calculated octanol/water partition coefficient, revealed that both chosen compounds have a consensus Log P value of less than 5, as shown in Table 7. Compounds with balanced lipophilicity levels are likely to be more effectively absorbed and able to penetrate biological membranes within organisms (Fonteh et al., 2015). The predictive water solubility of these phytochemicals were based on three models and they are : ESOL, Ali, and SILICOS-IT. The Log S (ESOL) values for Allicin (1.34) and Trigonelline (1.39) indicate better water solubility signifying their good metabolism in human body. This result aligns with the report of Sorkun et al., who reported that values between 0 and 2 suggest that a compound is soluble, values between 2 and 4 indicate that a compound has limited solubility and values below 4 suggest that a compound is insoluble (Sorkun, Khetan, & Er, 2019). Likewise, similar solubility pattern is noticed in Log S (Ali), in which Allicin have shown the excellent Log S (Ali) value of -2.20, succeeding by Trigonelline with a Log S (Ali) value of -1.00. In Log S (SILICOS-IT), allicin has a value of -1.70, and Trigonelline has -0.94, suggesting that Trigonelline is more soluble than Allicin according to these two methods.

Furthermore, the compounds under investigation exhibited high gastrointestinal absorption. This was demonstrated by their minimal interaction with permeability glycoprotein, by their moderate Log Kp values greater than 2.5 cm/s, and by their limited potential for skin penetration (Han et al., 2019).

The results presented in Table 8 suggest that only Allicin has the potential to cross the Blood-brain barrier (BBB), indicating a need for further investigation into allicins' potential toxicity. Furthermore, none of the compounds were found to inhibit CYP2C19, which implies that they may interfere with the metabolism of various therapeutic drugs, including those used against ulcer, malaria, seizures along with those used for anesthetic, and sedative purposes (Enmozhi, Raja, Sebastine, & Joseph, 2021). Both compounds also exhibited no significant inhibition effects on both CYP1A2 as well as CYP2D6, suggesting they might affect on the metabolism in liver and metabolism of certain types of drugs like Beta-blockers, antidepressants and drugs taken against metabolic syndrome disorder (Enmozhi et al., 2021). Additionally, neither com-

Table 7: Predictive physicohemical properties of Allicin and Trigonelline.

Properties	Allicin	Trigonelline
Molecular weight (g/mol)	162.27	137.14
Number of heavy atoms	9	27
Lipophilicity:		
Log $P_{o/w}$ (ILOGP)	1.95	-3.11
Log $P_{o/w}$ (XLOGP3)	1.31	0.51
Log $P_{o/w}$ (WLOGP)	2.62	-1.13
Log $P_{o/w}$ (MLOGP)	1.18	0.33
Log $P_{o/w}$ (SILICOS-IT)	0.96	0.36
Consensus Log $P_{o/w}$	1.61	-0.61
Water Solubility:		
Log S (ESOL)	-1.34	-1.39
Log S (Ali)	-2.20	-1.00
Log S (SILICOS-IT)	-1.70	-0.94

pound was capable of inhibiting CYP2C9 or CYP3A4, indicating they lack potency in blocking the oxidation process of the steroids, fatty acids, and xenobiotics, as well as in synthesis of the hormones and it's breakingdown (Enmozhi et al, 2021).

Table 8: Pharmacokinetics prediction properties of allicin and Trigonelline.

Properties	Allicin	Trigonelline
GIA absorption	High	High
BBB permeation	Yes	No
CYP1A2 inhibitor	No	No
CYP2B6 inhibitor	No	No
CYP2C19 inhibitor	No	No
CYP2D6 inhibitor	No	No
CYP3A4 inhibitor	No	No
Log K_p [skin permeation](cm/s)	-0.36	-6.77

Furthermore, the outcomes of the comparative evaluation of the theoretical drug-likeness of these compounds are shown in Figure 10 alongside in Table 9. While assessing the radar plot, it is revealed that Allicin fell inside the desired region i.e pink region, suggesting promising potential for Allicin as a candidate compound compatible for the drug making (Daina et al, 2017). This finding is consistent with Allicins' observed lipophilicity and water-solubility characteristics. In contrast, Trigonelline's radar plot deviated from the ideal range, but only at points of saturation. This indicates that while trigonelline may not be as well-suited for oral administration as Allicin, it still maintains some favorable properties 10.

On the basis of Lipinski's Rule of Five, to be adminstrated orally, drugs must agree with minimum three out of four standard set by this rule: the molecular mass of the compounds should be 500 Dalton or less; hydrogen bond acceptors should be equal to 10 or less than that; there

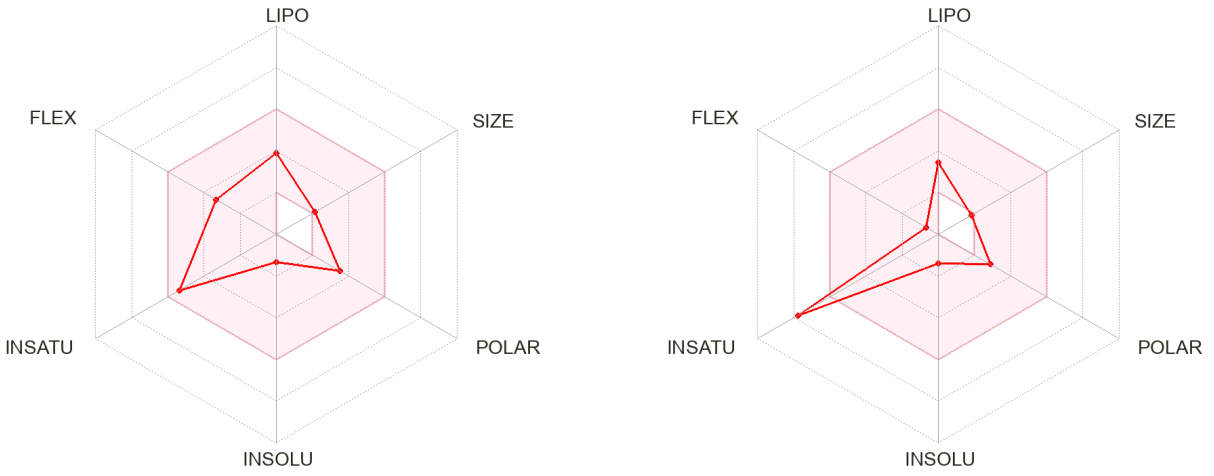

(a) **(b)**

Figure 11: Bioavaibility radar plot of (a) allicin and (b) Trigonelline.

should be 5 or fewer hydrogen bond donors should be equal to five or less than that ; and the octanol-water partition coefficient (LogP) should not be above 5 (or MlogP $\leq$ 5) (Lipinski, Lombardo, Dominy, & Feeney, 2012). As shown in Table 9, both compounds obeyed the standards outlined in Lipinski's Rule of Five, indicating them as the suitable candidates to be drugs. Additional assessments using a range of drug-likeness filters, including those proposed by Ghose, Veber, Egan, and Muegge, have been conducted to evaluate the compounds. These evaluations confirm that the compounds meet the criteria set forth by the Veber and Egan rules, indicating their suitability in terms of drug-likeness according to these standards. But both the compounds failed to set standard established by Ghose and Muegge. This discrepancy is due to the fact that the compounds have fewer than 20 heavy atoms and molecular weights that fall below 200 g/mol. As a result, they do not meet the specifications outlined by Ghose and Muegge, which take into account these specific molecular parameters (Daina et al., 2017).

Table 9: Predictive Drug-likeness of Allicin and Trigonelline.

Criterion	Allicin	Trigonelline
Lipinski	Yes	Yes
Ghose	No	No
Veber	Yes	Yes
Egan	Yes	Yes
Muegge	No	No
Bioavailability score	0.55	0.55

The BOILED-Egg model forecasts that molecules will be absorbed by the gastrointestinal tract if they fall within the white zone and can cross the blood-brain barrier if they are within the yellow zone. This prediction is based on their lipophilicity (WLOGP) and polarity (TPSA) (Daina et al., 2017). Like depicted in the Figure 13, the Trigonelline is situated in the white

region marked in red, indicating a higher likelihood of gastrointestinal absorption, and it is actively effluxed by P-glycoprotein (PGP+). Conversely, the Allicin molecule, shown in Figure 12, resides inside the yellow zone, suggesting a greater probability of passive diffusion by the blood-brain barrier, while also being actively effluxed by P-glycoprotein (PGP+). This model provides insight into the absorption and permeability characteristics of these molecules, indicating their potential bioavailability and interactions within the body (Daina et al, 2017).

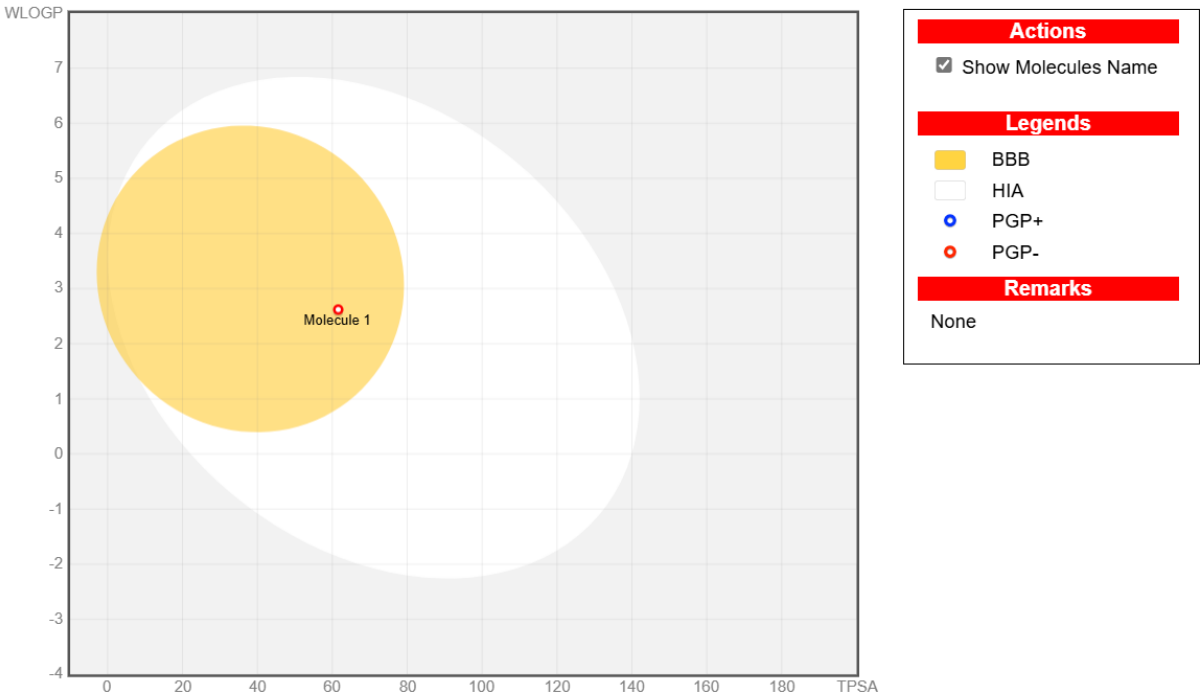

Figure 12: Boiled egg image representation of Allicin.

Toxic doses are commonly represented by LD50 values (mg/kg body weight). Compounds with LD50 values between 1000 mg/kg and 5000 mg/kg are classified as having low to moderate toxicity (Herkenne et al, 2008). The computational toxicological analysis of allicin and trigonelline revealed that the median lethal dose (LD50) values, representing the amount required to cause death in 50% of subjects, were moderately high for Allicin at 874 mg/kg and very high for Trigonelline at 3720 mg/kg (see Table 10). Under the Globally Harmonized System of Classification and Labeling of Chemicals (GHS), Allicin and Trigonelline have been classified as categories 4 and 5, respectively, which reflects their moderate to very low toxicity (Herkenne et al, 2008).

The prediction of organ toxicity specifically hepatotoxicity, neurotoxicity, nephrotoxicity, respiratory toxicity, and cardiotoxicityrevealed that Allicin is inactive for all these, while Trigonelline could induce respiratory toxicity and neurotoxicity. Regarding the prediction of toxicity endpoints namely carcinogenicity, immunotoxicity, mutagenicity, cytotoxicity, BBB (blood-brain barrier) permeability, clinical toxicity, and nutritional toxicity, it was shown that both

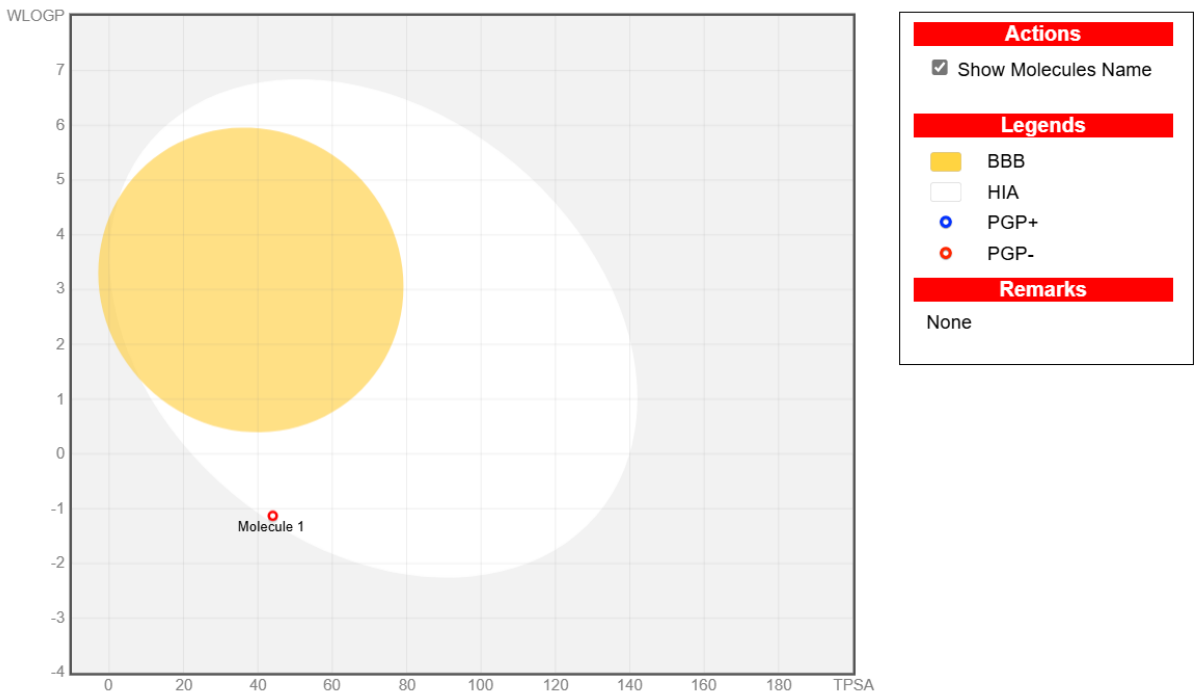

Figure 13: Boiled egg image representation of Trigonelline.

Table 10: Oral toxicity prediction results of Allicin and Trigonelline.

Properties	Allicin	Trigonelline
LD50 (mg/kg)	874	3720
Predicted Toxicity Class	4	5
Organ Toxicty:		
Hepatotoxicity	Inactive	Inactive
Neurotoxicity	Inactive	Active
Nephrotoxicity	Inactive	Inactive
Respiratory Toxicity	Inactive	Active
Cardiotoxicity	Inactive	Inactive
Toxicity end points:		
Carcinogenicity	Inactive	Inactive
Immunotoxicity	Inactive	Inactive
Mutagenicity	Inactive	Inactive
Cytotoxicity	Inactive	Inactive
BBB-barrier	Active	Active
Ecotoxicity	Inactive	Active
Clinical toxicity	Inactive	Inactive
Nutritional toxicity	Inactive	Inactive

allicin and trigonelline could induce BBB permeability, while trigonelline could induce ecotoxicity. In the same respect, allicin and trigonelline have no toxicity effects when interacting with several biochemical pathways. Such pathways include; Aryl hydrocarbon receptor that plays a role in the reaction to toxins in the environment; Androgen receptor that has functions in male sexual characteristics and reproduction; Aromatase which is a vital enzyme in estro-

gen production. They also integrate safely the estrogen receptor on account of the estrogen hormone impacts, the nuclear factor (erythroid-derived 2) like antioxidant responsive element fundamental in the control of oxidative stress, and the heat shock factor response element which is of crucial benefit to the synthesis of protein and cellular stress (Atkins, De Paula, & Keeler, 2018). Furthermore, it is also shown that these compounds hardly influence the mitochondrial membrane potential that is critical to energy production or tumor suppressor proteins need for the regulation of cell division and to avoid tumor formation (Atkins et al, 2018).

CHAPTER 5

5. CONCLUSIONS AND RECOMMENDATION

5.1 Conclusions

Ultimately, a DFT study and ADME-Toxicity evaluation of two phytochemicals Allicin and Trigonelline focusing on their stability, reactivity, and interaction within biological systems, was performed. Our findings indicate that Allicin exhibits comparatively higher stability, while Trigonelline shows a higher dipole moment, suggesting greater reactivity. The nucleophilic and electrophilic reaction sites of these molecules were predicted using MEP surface analysis, and Mulliken atomic charges were also examined and analyzed. Allicin has a larger HOMO-LUMO gap, refering it as having relatively lower reactivity than Trigonelline. However, the lower ionization potential of Trigonelline indicates a higher electron-donating capacity, positioning it as a better candidate for antioxidant activity between the two. Additionally, Trigonelline was found to be softer and more electrophilic than Allicin.

The ADMET analysis reveals that both compounds exhibit suitable lipophilicity and solubility, with Trigonelline being more soluble, while both show good gastrointestinal absorption. The radar plot analysis showed that Allicin falls within the desired range (the pink region), indicating its promising potential as a candidate for drug development. In contrast, Trigonelline's radar plot slightly deviated from the ideal range, primarily at saturation points, suggesting that while Trigonelline may not be as well-suited for oral administration as Allicin, it still possesses some favorable properties. Two of two compounds fulfill the requirements of Lipinski's Rule of Five, this suggested that they have potential to be drug. Additionally, the LD50 values suggest that these compounds may have low toxicity, which is negligible. The pharmacokinetics and toxicity studies further confirmed that both compounds exhibit good drug-likeness and trigger negligible toxicity in the human beings.

The theoretical results we obtained correspond closely with the experimental findings from similar studies conducted earlier. Thus, I anticipate that the quantum chemical calculations and ADMET analysis performed on these two phytochemicals will be highly valuable for understanding their overall activity, bioactivity, and drug-likeness. These *in silico* outcomes will also aid in designing further experiments and predicting potential results.

Additional *in vitro* experiments and preclinical trials are needed to validate the anticipated outcomes.

5.2 Novelty and National Prosperity aspect of Project work

This research introduces a novel approach by integrating DFT studies and ADMET analysis under one framework to explore the bioactivity and drug-likeness of two prominent phytochemicals, Allicin and Trigonelline. The combined use of Density Functional Theory (DFT) and ADME-Toxicity evaluations offers a comprehensive analysis of these compounds' electronic properties, stability, and interactions within biological systems. This distinctive approach provides new insights into the potential therapeutic applications and safety profiles of Allicin and Trigonelline, which have largely been unexplored in such a detailed and hybrid computational context.

The novelty of this study lies in its comparative analysis of Allicin and Trigonelline, two naturally occurring compounds commonly found in foods consumed daily and possessing significant medicinal properties. By conducting a thorough DFT analysis and ADMET evaluation, this research contributes to a deeper understanding of their potential as drug candidates.

In the context of the widespread prevalence of chronic diseases caused by metabolic syndrome disorders like diabetes, hypertension, and high uric acid, which are common in the South Asian region due to a lack of balanced diets and health awareness, the exploration of phytochemicals like Allicin and Trigonelline becomes crucial. Additionally, oxidative stress and inflammation are causing numerous health issues, and cancer treatments have not yet been effectively established. This research which is based on the compounds, known for their therapeutic benefits such as anti-carcinogenic, anti-diabetic, anti-inflammatory, antioxidant, and antihypertensive properties do have potential for a lot of research and the possibility of unveiling new methods to fight these chronic illnesses.

This research, based in computational biophysics, not only enhances the scientific knowledge base but also aligns with national priorities in advancing drug discovery and development, as well as combating chronic illnesses that have impacted millions of lives across the country and the world. The findings from this study hold promise for improving public health by identifying safer and more effective natural alternatives for treating chronic diseases, thus contributing to national health prosperity. Furthermore, the results can stimulate further research and development in the sector of pharmaceutical development using herbal products, supporting the country's goals of fostering innovation and achieving self-reliance in medicinal research, especially given the country's rich potential in herbal medicine.

5.3 Limitations of the work

Taking into the account about the valuable insights in the electronic properties, ADME characteristics, and toxicity profiles of Allicin and Trigonelline provided by this research, several limitations must be acknowledged:

1. The DFT calculations and ADME predictions rely on selected models and parameters, which might not fully capture all interactions or properties.

2. Theoretical results require experimental verification through laboratory and live organism studies to establish their biological relevance and therapeutic importance..

3. Predictions from tools like SwissADME and ProTox may not account for all physiological variations, and the absence of docking studies may limit insights into potential interactions with biological targets.

4. The study focused on Allicin and Trigonelline only, without comparing a broader range of compounds, and was limited by available computational resources. Molecular dynamics simulations could provide additional insights.

5.4 Recommendations for further project

The dimensions of structure, electronic properties, and vibrational characteristics of both molecules have been assesed computationally using DFT methods with Gaussian, while ADMET characteristics were assessed using SwissADME and ProTox. Hence, the findings from this research may require experimental verification as well.

Further, the work contains the basic essential properties of potential drugs. Thus, these findings can be helpful in seeking these compounds for drug usage and therapeutic applications. The recommendations for further work are stated below:

1. With the identification of some of the enzymes, receptors, and nucleic acids corresponding to the therapeutic benefits these two molecules pose, their interactions with those enzymes can be studied using molecular docking simulations and docking studies.

2. For exploring the antioxidant properties of these molecules in more detail, studies of Allicin and Trigonelline with structural modifications can be performed.

3. For the prediction of the the binding affinity and stability of Allicin and Trigonelline with various biological targets and to get deeper insights into their interaction mechanisms, the computational studies should be extended to include Molecular Dynamics (MD) simulations and docking studies with different targets from the human body.

4. The research can be further extended to other phytochemicals with similar structures or properties, conducting comparative studies alongside these compounds.

REFERENCES

Adekoya, O. C., Adekoya, G. J., Sadiku, E. R., Hamam, Y., & Ray, S. S. (2022). Application of dft calculations in designing polymer-based drug delivery systems: An overview. *Pharmaceutics*, *14*(9), 1972.

Aktar, S., Ferdousi, F., Kondo, S., Kagawa, T., & Isoda, H. (2024). Transcriptomics and biochemical evidence of trigonelline ameliorating learning and memory decline in the senescence-accelerated mouse prone 8 (samp8) model by suppressing proinflammatory cytokines and elevating neurotransmitter release. *GeroScience*, *46*(2), 1671–1691.

Allred, K. F., Yackley, K. M., Vanamala, J., & Allred, C. D. (2009). Trigonelline is a novel phytoestrogen in coffee beans. *The Journal of nutrition*, *139*(10), 1833–1838.

Atkins, P., De Paula, J., & Keeler, J. (2018). *Atkins' physical chemistry*. Oxford University Press. Retrieved from https://books.google.com.np/books?id=3QpDDwAAQBAJ

Balani, S. K., Miwa, G. T., Gan, L.-S., Wu, J.-T., & Lee, F. W. (2005). Strategy of utilizing in vitro and in vivo adme tools for lead optimization and drug candidate selection. *Current topics in medicinal chemistry*, *5*(11), 1033–1038.

Banerjee, P., Kemmler, E., Dunkel, M., & Preissner, R. (2024). Protox 3.0: a webserver for the prediction of toxicity of chemicals. *Nucleic Acids Research*, gkae303.

Barim, E., & Akman, F. (2019). Synthesis, characterization and spectroscopic investigation of n-(2-acetylbenzofuran-3-yl) acrylamide monomer: Molecular structure, homo–lumo study, td-dft and mep analysis. *Journal of Molecular Structure*, *1195*, 506–513.

Becke, A. D. (1988). Density-functional exchange-energy approximation with correct asymptotic behavior. *Physical review A*, *38*(6), 3098.

Binkley, J. S., Pople, J. A., & Hehre, W. J. (1980). Self-consistent molecular orbital methods. 21. small split-valence basis sets for first-row elements. *Journal of the American Chemical Society*, *102*(3), 939–947.

Bitew, M., Desalegn, T., Demissie, T. B., Belayneh, A., Endale, M., & Eswaramoorthy, R. (2021). Pharmacokinetics and drug-likeness of antidiabetic flavonoids: Molecular docking and dft study. *Plos one*, *16*(12), e0260853.

Block, E. (1985). The chemistry of garlic and onions. *Scientific american*, *252*(3), 114–121.

Borah, B., & Devi, T. G. (2020). Characterization of zn (l-proline) 2 complex using spectroscopic techniques and dft analysis. *Journal of Molecular structure*, *1210*, 128022.

Borlinghaus, J., Albrecht, F., Gruhlke, M. C., Nwachukwu, I. D., & Slusarenko, A. J. (2014). Allicin: chemistry and biological properties. *Molecules and replica*, *19*(8), 12591–12618.

Bretonnet, J.-L. (2017). Basics of the density functional theory. *AIMS Materials Science*, *4*(6), 1372–1405.

Chan, J. Y.-Y., Yuen, A. C.-Y., Chan, R. Y.-K., & Chan, S.-W. (2013). A review of the car-

diovascular benefits and antioxidant properties of allicin. *Phytotherapy research*, *27*(5), 637–646.

Choo, S., Chin, V. K., Wong, E. H., Madhavan, P., Tay, S. T., Yong, P. V. C., & Chong, P. P. (2020). Antimicrobial properties of allicin used alone or in combination with other medications. *Folia Microbiologica*, *65*, 451–465.

Daglia, M., Cuzzoni, M. T., & Dacarro, C. (1994). Antibacterial activity of coffee: relationship between biological activity and chemical markers. *Journal of Agricultural and Food Chemistry*, *42*(10), 2273–2277.

Daina, A., Michielin, O., & Zoete, V. (2017). Swissadme: a free web tool to evaluate pharmacokinetics, drug-likeness and medicinal chemistry friendliness of small molecules. *Scientific reports*, *7*(1), 42717.

Demircioğlu, Z., Kaştaş, Ç. A., & Büyükgüngör, O. (2015). Theoretical analysis (nbo, npa, mulliken population method) and molecular orbital studies (hardness, chemical potential, electrophilicity and fukui function analysis) of (e)-2-((4-hydroxy-2-methylphenylimino) methyl)-3-methoxyphenol. *Journal of Molecular structure*, *1091*, 183–195.

Drwal, M. N., Banerjee, P., Dunkel, M., Wettig, M. R., & Preissner, R. (2014). Protox: a web server for the in silico prediction of rodent oral toxicity. *Nucleic acids research*, *42*(W1), W53–W58.

Enmozhi, S. K., Raja, K., Sebastine, I., & Joseph, J. (2021). Andrographolide as a potential inhibitor of sars-cov-2 main protease: an in silico approach. *Journal of biomolecular structure and dynamics*, *39*(9), 3092–3098.

Fonteh, P., Elkhadir, A., Omondi, B., Guzei, I., Darkwa, J., & Meyer, D. (2015). Impedance technology reveals correlations between cytotoxicity and lipophilicity of mono and bimetallic phosphine complexes. *Biometals*, *28*, 653–667.

Fouad, R., & Adly, O. M. (2021). Novel cu2+ and zn2+ nanocomplexes drug based on hydrazone ligand bearings chromone and triazine moieties: Structural, spectral, dft, molecular docking and cytotoxic studies. *Journal of Molecular Structure*, *1225*, 129158.

Frisch, A., et al. (2009). gaussian 09w reference. *Wallingford, USA, 25p*, *470*.

Gao, Y., Wang, B., Qin, G., Liang, S., Yin, J., Jiang, H., ... Li, X. (2024). Therapeutic potentials of allicin in cardiovascular disease: advances and future directions. *Chinese Medicine*, *19*(1), 93.

García-Trejo, E. M., Arellano-Buendía, A. S., Argüello-García, R., Loredo-Mendoza, M. L., García-Arroyo, F. E., Arellano-Mendoza, M. G., ... others (2016). Effects of allicin on hypertension and cardiac function in chronic kidney disease. *Oxidative medicine and cellular longevity*, *2016*(1), 3850402.

Gökalp, F. (2018). The inhibition effect of garlic-derived compounds on human immunodeficiency virus type 1 and saquinavir. *Journal of Biochemical and Molecular Toxicology*, *32*(11), e22215.

Greenwell, M., & Rahman, P. (2015). Medicinal plants: their use in anticancer treatment.

International journal of pharmaceutical sciences and research, *6*(10), 4103.

Gruhlke, M. C., & Slusarenko, A. J. (2012). The biology of reactive sulfur species (rss). *Plant Physiology and Biochemistry*, *59*, 98–107.

Gunasekaran, S., Balaji, R. A., Kumeresan, S., Anand, G., & Srinivasan, S. (2008). Experimental and theoretical investigations of spectroscopic properties of n-acetyl-5-methoxytryptamine. *Can. J. Anal. Sci. Spectrosc*, *53*(4), 149–162.

Han, Y., Zhang, J., Hu, C. Q., Zhang, X., Ma, B., & Zhang, P. (2019). In silico adme and toxicity prediction of ceftazidime and its impurities. *Frontiers in pharmacology*, *10*, 434.

Haneef, J., Amir, M., Sheikh, N. A., & Chadha, R. (2023). Mitigating drug stability challenges through cocrystallization. *AAPS PharmSciTech*, *24*(2), 62.

Hartree, D. R. (1928). The wave mechanics of an atom with a non-coulomb central field. part i. theory and methods. In *Mathematical proceedings of the cambridge philosophical society* (Vol. 24, pp. 89–110).

Hehre, W. J., Ditchfield, R., & Pople, J. A. (1972). Selfconsistent molecular orbital methods. xii. further extensions of gaussiantype basis sets for use in molecular orbital studies of organic molecules. *The Journal of Chemical Physics*, *56*(5), 2257–2261.

Henry Anderson, T. (1949). *The plant alkaloids* (4th ed.). Philadelphia: The Blakiston Company.

Herkenne, C., Alberti, I., Naik, A., Kalia, Y. N., Mathy, F.-X., Préat, V., & Guy, R. H. (2008). In vivo methods for the assessment of topical drug bioavailability. *Pharmaceutical research*, *25*, 87–103.

Hohenberg, P., & Kohn, W. (1964). Inhomogeneous electron gas, physical review, 136, 3b. *B864–B871*.

Issaoui, N., Ghalla, H., Muthu, S., Flakus, H., & Oujia, B. (2015). Molecular structure, vibrational spectra, aim, homo–lumo, nbo, uv, first order hyperpolarizability, analysis of 3-thiophenecarboxylic acid monomer and dimer by hartree–fock and density functional theory. *Spectrochimica acta part a: molecular and biomolecular spectroscopy*, *136*, 1227–1242.

Jensen, F. (2007). Electronic structure methods: Independent particle models. *Introduction to computational chemistry*, *2*, 80–132.

Koch, H. P., & Lawson, L. D. (1996). Garlic: the science and therapeutic application of allium sativum l. and related species. *Williams & Wilkins*.

Kohn, W., Becke, A. D., & Parr, R. G. (1996). Density functional theory of electronic structure. *The journal of physical chemistry*, *100*(31), 12974–12980.

Kohn, W., & Sham, L. J. (1965). Self-consistent equations including exchange and correlation effects. *Physical review*, *140*(4A), A1133.

Kourounakis, P., & Rekka, E. (1991). Effect on active oxygen species of alliin and allium sativum (garlic) powder. *Research communications in chemical pathology and pharma-*

cology, *74*(2), 249–252.

Krishnan, R., Binkley, J. S., Seeger, R., & Pople, J. A. (1980). Self-consistent molecular orbital methods. xx. a basis set for correlated wave functions. *The Journal of chemical physics*, *72*(1), 650–654.

Kudin, K. N., & Scuseria, G. E. (2000). Linear-scaling density-functional theory with gaussian orbitals and periodic boundary conditions: Efficient evaluation of energy and forces via the fast multipole method. *Physical Review B*, *61*(24), 16440.

Kumar, P. S., Vasudevan, K., Prakasam, A., Geetha, M., & Anbarasan, P. (2010). Quantum chemistry calculations of 3-phenoxyphthalonitrile dye sensitizer for solar cells. *Spectrochimica Acta Part A: Molecular and Biomolecular Spectroscopy*, *77*(1), 45–50.

Lien, E. J., Guo, Z.-R., Li, R.-L., & Su, C.-T. (1982). Use of dipole moment as a parameter in drug–receptor interaction and quantitative structure–activity relationship studies. *Journal of pharmaceutical sciences*, *71*(6), 641–655.

Lipinski, C. A., Lombardo, F., Dominy, B. W., & Feeney, P. J. (2012). Experimental and computational approaches to estimate solubility and permeability in drug discovery and development settings. *Advanced drug delivery reviews*, *64*, 4–17.

Mishra, R., Joshi, B. D., Srivastava, A., Tandon, P., & Jain, S. (2014). Quantum chemical and experimental studies on the structure and vibrational spectra of an alkaloid–corlumine. *Spectrochimica Acta Part A: Molecular and Biomolecular Spectroscopy*, *118*, 470–480.

Nguyen, V., Taine, E. G., Meng, D., Cui, T., & Tan, W. (2024). Pharmacological activities, therapeutic effects, and mechanistic actions of trigonelline. *International Journal of Molecular Sciences*, *25*(6), 3385.

Nogrady, T., & Weaver, D. F. (2005). *Medicinal chemistry: a molecular and biochemical approach*. Oxford University Press.

Noureddine, O., Issaoui, N., & Al-Dossary, O. (2021). Dft and molecular docking study of chloroquine derivatives as antiviral to coronavirus covid-19. *Journal of King Saud University-Science*, *33*(1), 101248.

Ojha, L. K., Tüzün, B., & Bhawsar, J. (2020). Experimental and theoretical study of effect of allium sativum extracts as corrosion inhibitor on mild steel in 1 m hcl medium. *Journal of bio-and tribo-corrosion*, *6*, 1–10.

Oso, B. J., Adeoye, A. O., & Olaoye, I. F. (2022). Pharmacoinformatics and hypothetical studies on allicin, curcumin, and gingerol as potential candidates against covid-19-associated proteases. *Journal of Biomolecular Structure and Dynamics*, *40*(1), 389–400.

Ouzir, M., El Bairi, K., & Amzazi, S. (2016). Toxicological properties of fenugreek (trigonella foenum graecum). *Food and Chemical Toxicology*, *96*, 145–154.

Padmanabhan, J., Parthasarathi, R., Subramanian, V., & Chattaraj, P. (2007). Electrophilicity-based charge transfer descriptor. *The Journal of Physical Chemistry A*, *111*(7), 1358–1361.

Parr, R. G., Szentpály, L. v., & Liu, S. (1999). Electrophilicity index. *Journal of the American*

Chemical Society, *121*(9), 1922–1924.

Pearson, R. G. (1988). Absolute electronegativity and hardness: application to inorganic chemistry. *Inorganic chemistry*, *27*(4), 734–740.

Perdew, J. P. (1986). Density-functional approximation for the correlation energy of the inhomogeneous electron gas. *Physical review B*, *33*(12), 8822.

Pereira, F., & Aires-de Sousa, J. (2018). Machine learning for the prediction of molecular dipole moments obtained by density functional theory. *Journal of cheminformatics*, *10*, 1–11.

Rahman, M. S. (2007). Allicin and other functional active components in garlic: Health benefits and bioavailability. *International Journal of Food Properties*, *10*(2), 245–268.

Ranjan, R., Choudhary, R. K., Singh, R. K., et al. (2023). Comparative assessment of physicochemical properties of plant active molecules having antidiabetic potential. *International Journal of Science and Research Archive*, *10*(2), 968–975.

Raymond Tice, P. (2000). *Trigonelline [535-83-1] review of toxicological literature* (Tech. Rep.). Research Triangle Park, North Carolina 27709: Integrated Laboratory Systems. (Prepared for Errol Zeiger, Ph.D., National Institute of Environmental Health Sciences, Contract No. N01-ES-65402)

Rishton, G. M. (2008). Natural products as a robust source of new drugs and drug leads: past successes and present day issues. *The American journal of cardiology*, *101*(10), S43–S49.

Rodriguez-Clemente, E., Gonzalez-Rodriguez, J., Valladarez-Cisneros, M., Chacon-Nava, J., Flores-De los Ríos, J., & Rodriguez-Valdez, L. (2017). Experimental and theoretical evaluation of allicin as corrosion inhibitor for carbon steel in sulfuric acid. *Journal of Materials and Environmental Sciences*, *8*(11), 3817–33.

Saikat, A. S. M., Hossain, R., Mina, F. B., Das, S., Khan, I. N., Mubarak, M. S., & Islam, M. T. (2021). Antidiabetic effect of garlic. *Revista Brasileira de Farmacognosia*, 1–11.

Salahub, D. R., Fournier, R., Młynarski, P., Papai, I., St-Amant, A., & Ushio, J. (1991). Gaussian-based density functional methodology, software, and applications. In *Density functional methods in chemistry* (pp. 77–100). Springer.

Schrödinger, E. (1926). Quantisierung als eigenwertproblem. *Annalen der physik*, *385*(13), 437–490.

Sherrill, C. D. (2000). An introduction to hartree-fock molecular orbital theory. *School of Chemistry and Biochemistry Georgia Institute of Technology*.

Slater, J. C. (1937). Wave functions in a periodic potential. *Physical Review*, *51*(10), 846.

Snape, T. J., Astles, A. M., & Davies, J. (2010). Understanding the chemical basis of drug stability and degradation. *Pharmaceutical journal*, *285*(7622), 416–417.

Sorkun, M. C., Khetan, A., & Er, S. (2019). Aqsoldb, a curated reference set of aqueous solubility and 2d descriptors for a diverse set of compounds. *Scientific data*, *6*(1), 143.

Taghour, M. S., Elkady, H., Eldehna, W. M., El-Deeb, N., Kenawy, A. M., Elkaeed, E. B., ...

others (2022). Design, synthesis, anti-proliferative evaluation, docking, and md simulations studies of new thiazolidine-2, 4-diones targeting vegfr-2 and apoptosis pathway. *PLoS One*, *17*(9), e0272362.

Tayyem, M. T., & Almatarneh, M. H. (2016). A dft computational study of the antioxidant activities exhibited by3-aryl-4-hydroxycoumarin derivatives. *J Chem Appl Biochem*, *3*, 119.

Tetko, I. V., Bruneau, P., Mewes, H.-W., Rohrer, D. C., & Poda, G. I. (2006). Can we estimate the accuracy of adme–tox predictions? *Drug discovery today*, *11*(15-16), 700–707.

Wani, T. A., Bhat, I. A., Guleria, K., Fayaz, M., Anju, T., Haritha, K., ... Kaloo, Z. A. (2022). Phytochemicals: Diversity, sources and their roles. In M. K. Swamy & A. Kumar (Eds.), *Phytochemical genomics: Plant metabolomics and medicinal plant genomics* (pp. 3–33). Singapore: Springer Nature Singapore. Retrieved from https://doi.org/10.1007/978-981-19-5779-6_1 doi: 10.1007/978-981-19-5779-6_1

Wu, F., Zhou, Y., Li, L., Shen, X., Chen, G., Wang, X., ... Huang, Z. (2020). Computational approaches in preclinical studies on drug discovery and development. *Frontiers in chemistry*, *8*, 726.

Yarnell, E. (2015, 02). Herbs for diabetes: Updatepart 2. *Alternative and Complementary Therapies*, *21*, 32-38. doi: 10.1089/act.2015.21104

Yatoo, M. I., Dimri, U., Gopalakrishnan, A., Karthik, K., Gopi, M., Khandia, R., ... others (2017). Beneficial health applications and medicinal values of pedicularis plants: A review. *Biomedicine & Pharmacotherapy*, *95*, 1301–1313.

Yavuz, S. Ç. (n.d.). Molecular docking and reactive sites identification (homo–lumo, mep) of allicin and diallyl disulfide: Potential anticancer inhibitor. *Karadeniz Fen Bilimleri Dergisi*, *13*(4), 1523–1539.

Zhou, J., Chan, L., & Zhou, S. (2012). Trigonelline: a plant alkaloid with therapeutic potential for diabetes and central nervous system disease. *Current medicinal chemistry*, *19*(21), 3523–3531.

Zhou, T., Huang, D., & Caflisch, A. (2010). Quantum mechanical methods for drug design. *Current topics in medicinal chemistry*, *10*(1), 33–45.

Zhou, Y., Li, X., Luo, W., Zhu, J., Zhao, J., Wang, M., ... Wang, B. (2022). *Allicin in digestive system cancer: from biological effects to clinical treatment.* (Vol. 13).

त्रिभुवन विश्वविद्यालय
Tribhuvan University

Ph. No. +977-014244047

त्रि–चन्द्र बहुमुखी क्याम्पस
Tri-Chandra Multiple Campus

स्थापित १९७५ वि.सं./Estd. 1918 A.D.

क्याम्पस प्रमुखको कार्यालय
Office of the Campus Chief

सरस्वती सदन, घण्टाघर, काठमाडौं, नेपाल
Saraswati Sadan, Ghantaghar, Kathmandu, Nepal

पत्र संख्या/Ref. No.:- .....

TRI-CHANDRA MULTIPLE CAMPUS 1918 A.D. SARASWATI-SADAN KATHMANDU

Date: 18/09/2024

Plagiarism Test Report

The B.Sc project entitled **"In Silico Study of Allicin and Trigonelline: Bioactivity and Drug-Likeness Through DFT and ADMET Analysis"** submitted by **Bishal Budha** for a plagiarism test on 14/09/2024, has been checked by the iThenticate plagiarism checker software. The software found an overall similarity index of 9% based on the following criteria.

Criteria:s

- Phrases - Excluded
- Quotes - Excluded
- Bibliography - Excluded
- Small Sources - Percentage(Zero)
- Small Match - 10 Words
- Abstract - Included
- Methods and Materials - Included

Please note that the similarity index generated by software may not fully reflect the quality and standards of the document. Therefore, it is strongly recommended that the respective authority manually review the checked file to ensure that the file meets the necessary standards of being well-written, well- researched, and maintaining academic integrity.

.....
Authorized Signature

Head of Department
Physics Department
Trichandra Multiple Campus

IN SILICO STUDY OF ALLICIN AND TRIGONELLINE: BIOACTIVITY AND DRUG-LIKENESS THROUGH DFT AND ADMET ANALYSIS

ORIGINALITY REPORT

9%
SIMILARITY INDEX

Checked by Rahul Nepal 15/09

PRIMARY SOURCES

1	journals.plos.org Internet	105 words — 1%
2	www.aimspress.com Internet	95 words — 1%
3	www.tandfonline.com	82 words — 1%
4	"Density Functional Theory", Computational Chemistry and Molecular Modeling, 2008	47 words — < 1%
5	docslib.org Internet	43 words — < 1%
6	www.mdpi.com	41 words — < 1%
7	Akinwunmi O. Adeoye, John A. Falode, Olabimpe C. Oladipupo, Tajudeen O. Obafemi, Babatunde J. Oso, Ige F. Olaoye. " Modulation of mitochondrial permeability transition pore opening by Myricetin and prediction of its-drug-like potential using approach ", Drug and Chemical Toxicology, 2022 Crossref	33 words — < 1%

21 words — < 1%

17 www.science.gov
Internet
21 words — < 1%

18 asianpubs.org
20 words — < 1%

19 vdoc.pub
20 words — < 1%

20 www.diva-portal.org
20 words — < 1%

21 Skripnyak, Natalia. "Theoretical Description of Ti and Ti Alloys from First Principles", Linkopings Universitet (Sweden), 2024
19 words — < 1%

22 Vimal K. Maurya, Swatantra Kumar, Madan L. B. Bhatt, Shailendra K. Saxena. "Antiviral activity of traditional medicinal plants from Ayurveda against SARS-CoV-2 infection", Journal of Biomolecular Structure and Dynamics, 2020
Crossref
19 words — < 1%

23 fdocument.org
Internet
18 words — < 1%

24 Chudzinski, Michael G., Corey A. McClary, and Mark S. Taylor. "Anion Receptors Composed of Hydrogen- and Halogen-Bond Donor Groups: Modulating Selectivity With Combinations of Distinct Noncovalent Interactions", Journal of the American Chemical Society, 2011.
17 words — < 1%

14 words — < 1%

34 Wolfram Koch, Max C. Holthausen. "A Chemist's Guide to Density Functional Theory", Wiley, 2001 — 13 words — < 1%
Crossref

35 core.ac.uk — 13 words — < 1%
Internet

36 kuscholarworks.ku.edu — 13 words — < 1%

37 services.chm.unipg.it — 13 words — < 1%

38 A. Hemanth Babu, D.S.N.B.K. Prasanth, Deepak A. Yaraguppi, Siva Prasad Panda et al. "Antiparkinson potential of khellin on retinone-induced Parkinson's disease in a zebrafish model: targeting MAO, inflammatory, and oxidative stress markers with molecular docking, MD simulations, and histopathology evidence", Comparative Biochemistry and Physiology Part C: Toxicology & Pharmacology, 2024 — 12 words — < 1%

39 Ramos, C.M.. "Density functional theory treatment of the structures and vibrational frequencies of 2,4- and 2,6-dinitrotoluenes", Journal of Molecular Structure: THEOCHEM, 20060914 — 12 words — < 1%
Crossref

40 archiv.ub.uni-heidelberg.de — 12 words — < 1%

41 d.docksci.com — 12 words — < 1%

42	ojs.ub.uni-konstanz.de Internet	12 words — < 1%
43	pubmed.ncbi.nlm.nih.gov Internet	12 words — < 1%
44	www.rsc.org Internet	12 words — < 1%
45	www2.fizik.usm.my Internet	12 words — < 1%
46	Anna De Masi, Pablo A. Ferrari, Errico Presutti. "Symmetric simple exclusion process with free boundaries", Probability Theory and Related Fields, 2014	11 words — < 1%
47	Maphisa, Xolani. "Numerical Simulations of Stress Induced sp2 -sp3 Transitions in Carbon Nanotubes", University of Johannesburg (South Africa), 2022 ProQuest	11 words — < 1%
48	Nguyen, Huan A.. "Optical Spectroscopy Analysis of the Physicochemical Properties of Poly(3-Hexylthiophene) (P3HT) Solutions Using Various Solvents Towards Controllable Formation of Polymeric Aggregates", The University of Alabama, 2023	11 words — < 1%
49	amsdottorato.unibo.it Internet	11 words — < 1%
50	d-nb.info Internet	11 words — < 1%
51	ddd.uab.cat Internet	11 words — < 1%

62 John BO Mitchell. "Informatics, machine learning and computational medicinal chemistry", Future Medicinal Chemistry, 03/2011 — 10 words — < 1%

63 Josefa Tolosa, Francisco J. Barba, Noelia Pallarés, Emilia Ferrer. "Mycotoxin Identification and In Silico Toxicity Assessment Prediction in Atlantic Salmon", Marine Drugs, 2020 — 10 words — < 1%
Crossref

64 Mohammad Kazem Rofouei, Reza Soleymani, Abolfazl Aghaei, Mahmoud Mirzaei. "Synthesis, vibrational, electrostatic potential and NMR studies of (E and Z) 1-(4-chloro-3-nitrophenyl)-3-(2-methoxyphenyl)triazene: Combined experimental and DFT approaches", Journal of Molecular Structure, 2016 — 10 words — < 1%

65 Rogério F. Costa, Antônio S. N. Aguiar, Igor D. Borges, Ricardo Ternavisk et al. "Effect of ortho- and para-chlorine substitution on hydroxychlorochalcone", Journal of Molecular Modeling, 2021 — 10 words — < 1%

66 Rolando Larico Mamani. "Propriedades físicas de impurezas de níquel em diamante", Universidade de Sao Paulo, Agencia USP de Gestao da Informacao Academica (AGUIA), 2003 — 10 words — < 1%
Crossref Posted Content

67 Sushama Kauthale, Sunil Tekale, Manoj Damale, Jaiprakash Sangshetti, Rajendra Pawar. "Synthesis, biological evaluation, molecular docking, and ADMET studies of some isoxazole-based amides", Medicinal Chemistry Research, 2017 — 10 words — < 1%

68	Unge, Mikael. "Molecular Electronics A Theoretical Study of Electronic Structure of Bulk and Interfaces", Linkopings Universitet (Sweden), 2024	10 words — < 1%
69	biblio.ugent.be	10 words — < 1%
70	dictionnaire.sensagent.leparisien.fr Internet	10 words — < 1%
71	dokumen.pub	10 words — < 1%
72	gyan.iitg.ac.in	10 words — < 1%
73	pharmacia.pensoft.net	10 words — < 1%
74	worldwidescience.org Internet	10 words — < 1%
75	www.ncbi.nlm.nih.gov	10 words — < 1%